5-1-2018

High Speed Wear of Gallium Nitride

Zeyuan Tian
Lehigh University, christian19941011@outlook.com

High Speed Wear of Gallium Nitride

By

Zeyuan Tian

A Thesis

Presented to the Graduate and Research Committee

of Lehigh University

in Candidacy for the Degree of

Master of Science

in

Mechanical Engineering

Lehigh University

(May 2018)

This thesis is accepted and approved in partial fulfillment of the requirements for the Master of Science.

_____

Date

_____

Prof. Brandon A. Krick

Thesis Advisor

_____

Prof. D. Gary Harlow

Chairperson of Department

Acknowledgements

Thank you to the entire Lehigh Tribology Laboratory, especially Dr. Brandon Krick, for taking me on for this project. Thanks to Guosong Zheng for providing some great ideas and sharing his experience and expertise. Thank you, Thomas Babuska and Cooper Atkinson, for helping me a lot during this project. Thank you to Zhaohua Chang, for collaborating and machining; I couldn't finish this thesis without them.

Table of contents

Table of figures

Table of tables

Abstract

This thesis observes the tribological properties of GaN at relatively high sliding speeds. We choose a model for a pin-on-disk and unit direction rotate sliding experiments. To fulfill that we assemble a new high speed tribometer and completed some successful tests. In the results of these tests, we can find several interesting tribological properties (coefficient of friction and wear rate) of GaN in relatively high speed and get some reliable information when the GaN sliding under some specific conditions. The results are compared to former tests on GaN in Lehigh tribology lab, and it is proved that the c-plane of GaN has a 60-degree periodical variation on wear rate. Also, we can record the highest and lowest wear rate on each different experiment and recorded the data working on the further researches of GaN. Focus on the high-speed parameters, and applied on difference loads, we also can use the slide surface of GaN to the further band bending researches.

1.Introduction

1.1 Material Tribology

Since Peter Jost coined “tribology” in 1966 in a report of the UK Department of Education and Science[1], tribology was formally defined as a science and engineering of interacting surfaces in relative motion and attracts more researchers. Although, the concept enunciated a new name which from the Greek word “tribos”[2], the rudimentary contents of tribology, friction and wear, are as old as history. It involves the laws of friction, lubrication, and wear, focus on study and applicants. As a highly interdisciplinary in physics, chemistry, materials science and engineering, tribology plays an important role, especially in industrial application.

The industrial aspects of tribology are significant. Driving wheels, brakes, clutches, etc., for productive friction; Writing with a pencil, machining, polishing, etc., for productive wear; in contrast, like engines, gears, seals, etc., for the unproductive friction and wear. These examples manifest the industrial significance of tribology. Consider into the time and resource consuming for industries, tribology is surprisingly an unignore part. According to some reports, only in United States, since 1966 losses due to ignorance of tribology amount about 4% of its gross national product which means about $200 billion dollars lost per year, meanwhile energy resources use appear as friction in different forms are around one-third of the world[3]. Therefore, the importance of friction reduction and wear control is self-evident. As Peter Jost said, the better tribological practices can fulfill to savings of about 1% of gross national product of an industrial nation[4].

According to a 2017 research about global energy consumption, costs, and emissions for the tribology, they show that approximately23% (119 Exajoule) of the world’s total energy consumption from tribological contacts;20% of energy consumption (103 Exajoule) is used to overcome friction; 3% (16 Exajoule) is used to reproduce worn parts and idle equipment on account of wear and wear-related failures. Through the development of new surface, materials, and lubrication technologies in vehicles to reduce friction and protect wear, machinery, and other energy losses because of friction and wear could potentially be decreased by around 18% in the short term (8 years) and by around 40% in the long term (15 years). Which means these savings on one hand, in the long term, would achieve to 1.4% of the GDP annually and 8.7% of the total energy consumption. On the other hand, in the short-term, the potential savings in the manufacturing and residential sectors are predicted to be around 10%. In addition, some advanced tribological technologies can decline the carbon dioxide splits globally by approximately 1,460 $MtCO_2$ and saving up to 450,000 million Euros in the short term. Decline the carbon dioxide emissions globally by approximately 3,140 Mt CO_2 and saving up to 970,000 million Euros in the long term[5].

Hence, combined with the materials discussed above, the tribology as a multidisciplinary and interdisciplinary science, range from macro to nano-scales, worth to do more researches in the three aspects in conclusion:

First, tribology integrates basic knowledge and applied technology into a broad area of science that includes familiar friction, wear, and lubrication. Its engineering applications include design for tribological construction, equipment, and products; control of frictional wear and wear throughout the life cycle; implementation of lubrication techniques and development of new lubricants.

Second, friction materials research is the forefront of engineering and technology focus. Including lubricants and greases, their tribologically-related properties and the proper use of these properties are indispensable for improving the quality of tribological designs as well as for improving the quality of their equipment, reducing operating costs, basic means to reducing environmental pollution, and prolonging service life. In recent decades, friction material has been a frontier topic in the field of material science, chemistry, and surface engineering, as well as a hot topic in physics, control engineering, etc.

Third, tribology has important economic value. In the design of buildings, equipment, and products, attaching importance and actively apply to tribological frontier scientific and technological knowledge, actively carry out tribological design, and improve construction, equipment and products in order to improve the performance and reliability of buildings, equipment and products also reduce operating costs in the market competitiveness, there is more far-reaching significance.

1.2Wearofceramics

Considering their high melting point, low density in some cases and chemical inertness, Ceramics become important contenders for use as bearing and seal materials[6].

The ceramic material is an inorganic non-metal material made of natural or synthetic compounds after being shaped and sintered at high temperature, also a one of the most important materials among inorganic non-metal materials that people pay attention to after non-metal materials. It has the common advantages of both metal materials and polymer materials. In the process of continuous modification, it has greatly improved its fragility. Ceramic materials are unique in the field of materials because of their excellent performance. They are highly valued by people and will play a very important role in the future social development.

Ceramic materials can be divided into: common ceramic materials, which are made of natural materials such as feldspar, clay, and quartz, which are typically silicate materials that are sintered. Ordinary ceramic materials are rich in source, low in cost and mature in technology, and can be divided into daily-use ceramics, architectural ceramics, and chemical ceramics according to performance characteristics and applications; Special ceramic materials, this material is mainly made of high-purity synthetic raw materials, made of precision controlled process forming sintering, with some special properties to meet various needs, its main components are oxide ceramics, nitrides Ceramics, cermet, etc. Nano-ceramics, no matter whether the raw materials used for advanced ceramics or the finished grains are micrometers, they are also called micro-ceramics. When the raw and finished grains reach the nano-scale, they will be the preparation of ceramics, ceramics, and ceramics. Learning and ceramic processes bring about mutations that open wider applications for ceramic materials.

1.3 Research in GaN

To design and produce materials with a low coefficient of friction and low wear rate is always a challenge for a wide range of working environment. Nitride base coatings which possess high hardness, low friction and wear rate[7–12] shows a solution for applicants on surface engineering. As the development of ternary nitride coatings, many researches and industrial interest are attracted recently, focus on some better film properties like great conductivity, good hardness, high wear resistance and melting point, and excellent corrosion protection, etc. Thus, methods to produce a binary nitride compound (e.g. TiN, GaN, VN, ZrN, MoN, SiN, etc.) or ternary nitride compound (e.g. TiAlN, TiVN, TiMoN, etc.) are enunciated.

Gallium nitride (GaN) is a binary III/V direct band gap semiconductor commonly used in light-emitting diodes since the 1990s[31].The research and application of GaN materials have become the forefront and hotspot of semiconductor research. It is a new semiconductor material for the development of microelectronic devices and optoelectronic devices. It is also called the third generation of semiconductor materials. It has wide direct band gaps, strong atomic bonds, high thermal conductivity, good chemical stability (almost no corrosion by any acid) and other properties and strong resistance to irradiation in optoelectronics, high-temperature high-power devices and high application of microwave microwave devices has broad prospects. The GaN crystal is generally a hexagonal wurtzite structure. It has 4 atoms in a cell, and its atomic volume is about half that of GaAs.

GaN is an extremely stable compound and is a hard, high-melting material. Features are as follows:

(1) High chemical stability. At room temperature, GaN is insoluble in water, acids, and alkalis, and dissolves in a hot alkaline solution at a very slow rate. NaOH, H_2SO_4 and H_3PO_4 can erode the poor quality GaN more quickly and can be used for defect detection of these low quality GaN crystals. GaN exhibits unstable characteristics at high temperatures under HCl or H_2 gas and is most stable under N_2 gas.

(2) High melting point. The melting point is about 1700°C.

(3) High degree of ionization. The highest among the group III-V compounds (0.5 or 0.43).

(4) High hardness. At atmospheric pressure, because of its high hardness, it is also a good coating material.

Based on these great properties, the GaN is in high-prevalence at technological and applications, especially in the research about its remarkable optoelectronic properties[32–36].

However, few studies on mechanical properties of GaN when compare to the electrical and optical properties, the lack of the understanding of the mechanical characteristics of GaN results in relatively few innovations taking advantage of these properties for device applications; thus, is essential for opening new applications to understand the mechanical properties of GaN-based semiconductors. Specifically, the elastic constants of GaN have been investigated[37–40], resulting in wide utilizations for research concerning the lattice mismatch and piezoelectric polarization

effect[41–45]. In addition, the mechanical properties such as the Young's modulus, hardness, and fracture toughness of GaN material have been extensively studied[46–52], providing essential information for various scientific applications requiring those experimentally obtained parameters. In comparison, the tribological properties of GaN and other III-Nitride materials are still lacking: there are no investigations of wear performance and mechanisms of GaN-based materials. The closest studies have been chemical mechanical polishing and nano scratch experiments[53,54], but these are still very different from sliding wear. GaN plays a key role in modern semiconductor industry; thus, it is crucial to understand its wear behavior and reliability.

Recently in our Lehigh tribology lab, Guosong Zeng. et al. did many researches on tribological properties of GaN and made some interesting achievements. They measure wear rates and friction coefficients of GaN, find that GaN has remarkable tribological properties with wear rates from 10^{-9} to 10^{-7} $mm^3/(Nm)$, which means an ultralow wear rate[55].

Based on tribological experiments and molecular static simulation model. They also explored the relationship between the tribological (friction and wear) properties of GaN and the crystallographic order and orientation. They measure the friction and wear in every direction (3 degree for every rotation) on the c-plane of GaN on a pin-on-disk experiment. Then they observed a 60° periodicity of wear rate and friction coefficient, which means that there is a strong crystallographic orientation dependence of the sliding properties of GaN. This phenomenon and the origin of this periodicity is rooted in the symmetry presented in wurtzite hexagonal lattice structure of III-nitrides. Also, they recorded some interesting data, and make people have a better understanding of the tribological properties on different crystal direction of GaN. According to the research, lowest wear rate is $0.6 \times 10^{-7} mm^3/Nm$ with $< 1\bar{1}00 >$, while the wear rate associated with $< 1\bar{2}10 >$had the highest wearrate of $1.4 \times 10^{-7} mm^3/Nm$. On the contrary, higher friction coefficient can be observed along $< 1\bar{1}00 >$, while lower friction coefficient always appeared along $< 1\bar{2}10 >$.To explain the low wear rate and the periodicity of wear rate, the molecular static simulation model is introduced. After the simulation and calculation of the energy between atoms. It shows that higher energy barrier along $< 0\bar{1}00 >$, direction results in more difficult removal process of the material, which in turn results in its lower wear rate.

The anisotropy of friction coefficient is much subtler than the anisotropy of wear rate. The anisotropy in friction likely comes from the same or similar energetic barriers derived from crystalline structure that governs wear. The results also revealed energetic barriers to sliding strongly linked to the sliding direction. This supports that the crystallographic orientation dependences of wear rate are attributed to the anisotropic energy barrier distribution on the c-plane surface of GaN[56]. During this research, the results also indicated the wear behavior of GaN is highly depends on the humidity. To know more about how the moisture dependent wear mechanisms of gallium nitride, wear tests were carried out in our lab on custom ball-on-flat, reciprocating tribometer mounted inside a glove box with controlled environment. From these tests, the wear rate for GaN has a significant dependence on humidity, ranging from 9×10^{-9} mm^3/Nm to 9.5×10^{-7} mm^3/Nm[57]. After some serious researches, our lab has a better knowledge of the tribological properties of GaN, however, as one of the most important semiconductor

materials in the optoelectronic area, we still eager to figure out the photoelectrical properties of GaN combined with tribological tests.

Motivated by that, our lab tests the GaN by adjusting the humidity, sliding cycles, and normal load, and shows sliding on the surface of GaN can permanently change the electric field, resulting in an increased degree of band bending by more than 0.5 eV. Still, the band bending of GaN can be controlled by these parameters mentioned above. And we term this shear-induced modification to the band states as "tribodoping"[58].

1.4 Motivation& Hypothesis

Based on the researches from our lab about the tribological properties of GaN, there are several other interesting factors worth to focus, such as temperature, speed, and load dependencies etc. Since there are some districts or situations, and these factors usually influenced in engineering applications and for some scholar theory. Meanwhile, in our lab, we already know some factors can controlled the band bending when sliding the surface of GaN, to extend the research about it, we want to know the band bending is whether controlled in other parameters or not. Therefore, combined with the former tribological properties we already found and the practical value, we are looking at two controlling factors on the experiments of GaN: speed and normal force.

To have a better understand of GaN tribological properties in these two factors, we are focus on high speed which can arrived at 3000 rpm around with different normal forces in a pin-on-disk experiment.

We are planning to use two different normal forces with different sliding speeds. And we hypothesis that, high speed will influence the wear rate and friction coefficients of GaN, also different of normal force will get different outcomes. And the wear rate probably has a periodicity, the different crystal direction performs different tribological properties in the high-speed condition.

2.Experiment

2.1 Scanning white light interferometer(SWLI)

The main function of the scanning white light interferometer: observation, analysis, application. Interferometers are optical instruments that use the principle of interference to measure the difference in optical path lengths to determine the physical quantities involved. Any change in the optical path difference between the two coherent beams will cause the movement of the interference fringes very sensitively, and the optical path change of a certain coherent light is caused by the geometric path it passes or the change of the refractive index of the medium, so by interference Changes in the movement of the fringes can measure the small changes in the geometric length or refractive index, and thus measure other physical quantities related to this. The accuracy of the optical path difference measurement determines the accuracy of the measurement. Each time the interference fringe moves by one fringe spacing, the optical path difference changes by one wavelength (~10-7 m), so the interferometer measures the optical path difference in units of the wavelength of the light wave. The high measurement accuracy is unmatched by any other measurement method.

Our lab uses the SWLI (Bruker ContourGT-K) from Bruker company, Profiler provides the highest performing non-contact surface measurements for laboratory research and production process control. As the pinnacle of ten generations of white light interferometer innovation and design, this metrology system delivers the highest vertical resolution over the industry's largest field of view. Key features include full automation, a large motorized X, Y, Z stage, tip/tilt in the head, and an integral air isolation table. Which shows in figure 1.

***Figure 1*: Scanning whit light interferometer**

2.2 Material

The GaN sample we used to be performed on the (0001)-plane of GaN coatings grown epitaxial with metal organic chemical vapor deposition (MOCVD) on single crystalline sapphire wafers, with a crystal direction of $< 1\bar{2}10 >$. And the counter sample are ruby ball probes made by myself. The diameter of ruby ball is 3 mm and the sample of GaN is 2 inches. The samples are show in figure 2 below.

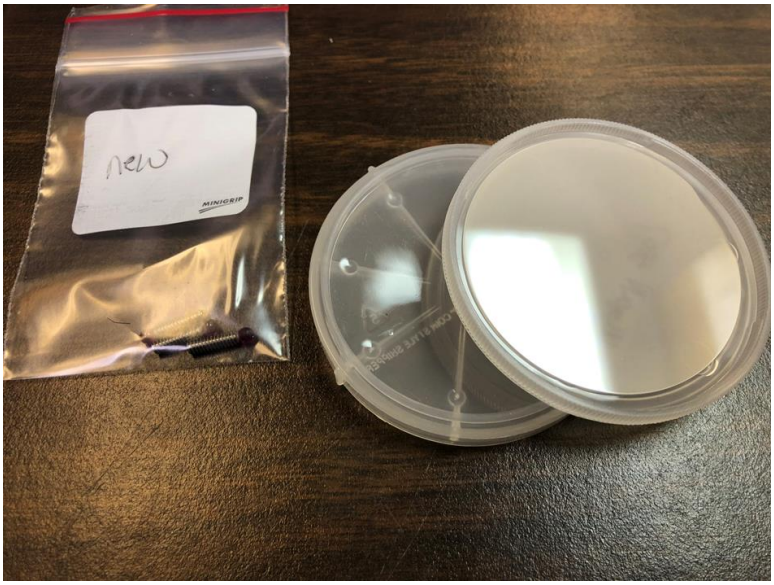

Figure 2:Ruby ball (left) and GaN (right)

When making probes, usually use glue to stick ruby ball and a little iron bar, thus there are few possible mistakes will let the glue covered the surface of ruby ball. To make sure the ruby ball is perfect, I used the SWLI to scan every ruby ball before I used, here are three figures of different situation of ruby balls, we can easily see the differences between the sapphires of ruby ball profiles. And the dirty one has a huge shade on the ball surface, which has epoxy on

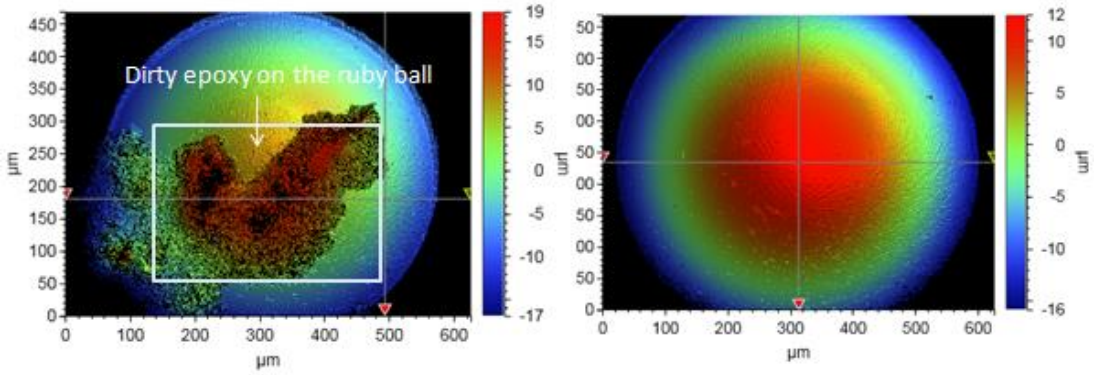

Figure 3: clean ruby ball profiles(right)and dirty ruby ball profiles (left)

Before used the sample of GaN, we need to clean the sample surface first, let the sample soaked in acetone with 10 minutes sonic then same procedures soaked in isopropanol. And the ultrasonic cleaner for sonic is bought from Branson.

2.3 Tribometer

2.3.1 Design equipment

The tribometer in our lab for this research called high speed pin-on-disk tribometer, it was original made based on high loads and high speed for bulk-on-disk to test metals, called rotary reciprocating tribometer, I designed and machined a plate and connected a cantilever to make an adaption, suitable for these experiments. The cantilever has two different directions micrometer, one is controlling the height, the other is controlling the distance. We can see the figure 5 to have a better understand of it.

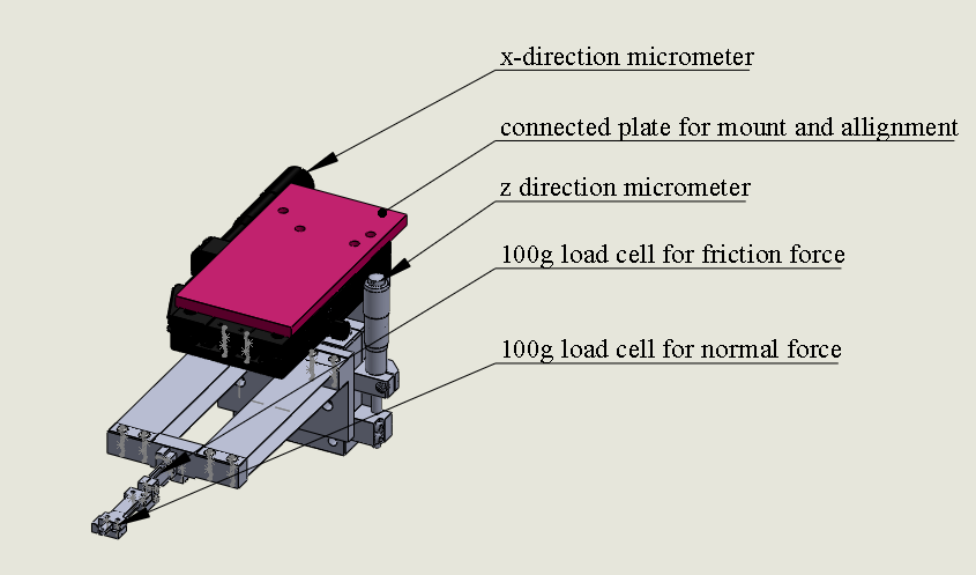

Figure 4: cantilever set on stage, the pic shows the x direction micrometer for controlling the x direction, z direction micrometer for controlling the height, the 100g load cells, and the designed plate for alignment the cantilever

Then turn the cantilever over and mount on original rotary tribometer shows on figure, it was made up by an alumina frame with an electric motor connected with a spin stage by belt, which can make the rotate speed arrives 3000 rpm or higher.

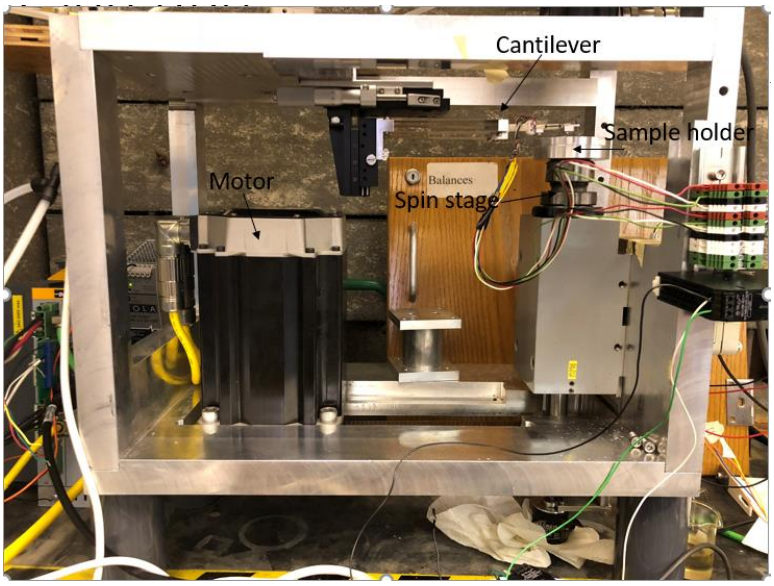

Figure 5: Rotary high speed tribometer, connected with cantilever, the figure shows the high-speed motor, the spin stage, the cantilever, sample holder, and the whole frame of the tribometer

2.3.2 Calibration

After setting up the equipment, there are two micrometers and a load cell need to be calibrated. First of all, we need to promise the probe screws on the cantilever is concentric on the sample holder when it mounted on the spin stage, still, we have to find the 0 position for the cantilever in x direction(horizontal), the first condition can fulfilled by machine a specific plate mentioned above to make sure the two center point on the same line; to find the 0 position for the x direction, I first set the x micrometer on a specific number of grid, and recorded the numbers, then use a metal probe to sliding on a sample of aluminum, after 1thound circles, there has a wear scar on the sample, appears as a circle, in figure 7, then with the help of SWLI scan software, I can easily get the radius of that circle. Then we can get a linear relationship between the micrometer grids and the actual radius. Using that method, we can find the 0 position on the micrometer, in this experiment, when the number of grids is 19, the radius equals to zero, which means the 0 position of x direction is found at 19 grids in micrometer.

Figure 6: the outer wear scar is sliding at 100 rpm, with 1000 circles

Then we still need to calibrate the normal forces and friction forces, read by two sensors connected with the load cell, that is to valuation a fraction on a Matlab code which can read and recorded every data on load cells. The method is let the load cell hang on several weights, 0.1, 0.5, and 1 N, then read the data of the normal forces on the Matlab, then simple average the data and find the linear relationship, we can get the fraction number of normal forces and friction forces.

After mounted all parts and completed the calibration, we can just start the experiment.

2.4 Methods

2.4.1 Parameters

Since the research is focus on the tribological properties for GaN in relatively high speed, I plan the sliding speeds are0.1m/s, 0.5m/s and 1m/s, and to make more comparison, I choose two different forces, 0.3N and 0.9N. When choosing the normal forces, there is one thing should be considered, that is we should keep the maximum normal forces smaller than around 10 percent of maximum Hertzian contact pressure. Also, the speed is so fast that can make some relatively big errors for normal force, therefore, we choose the maximum normal force equals 0.9N±50mN to make sure the force not surpass the 10 percent of the maximum Hertzian contact pressure. And we also should change radius to keep the sliding speeds same in different normal forces. The specific planning controlling parameters shows in table 2 and to promise the data are enough we

add another group of experiments shows in table 3. Considering into the time and experiment conditions there are four experiments are succeeded which shows in table 2 and plus the secondary experiments in table 3. Also, we need to notice that, the humidity, one factor also affects experiments outcomes[57], under 16% RH lab air in average. And the table 3 shows more specific for humidity in every single experiment.

F (N)	Diameter(mm)	Rpm	v(m/s)	cycles	t (minutes)
0.3	30.48	313.2971	0.5	100000	319.1858
0.9	33.02	289.1974	0.5	100000	345.7846
0.3	35.56	537.0808	1	100000	186.1917
0.9	38.1	501.2754	1	100000	199.4911

Table 1: The first planning controlling parameters

F(N)	Diameter(mm)	Rpm	v(m/s)	cycles	t(minutes)	humidity
0.3	10.16	187.9783	0.1	50000	265.9882	23%
0.9	12.7	150.3826	0.1	50000	332.4852	25%
0.3	15.24	626.5943	0.5	50000	79.79645	26%
0.9	17.78	537.0808	0.5	50000	93.09586	25%
0.3	20.32	939.8914	1	50000	53.19764	23%
0.9	22.86	835.459	1	50000	59.84734	28%

Table 2: The second controlling parameters

2.4.2 Calculation and data analysis

From these experiments we can get the data about the normal forces, friction force and spending time recorded by Matlab code on every circle. Also, we can easily get the coefficient of friction using $F = \mu N$, recorded by Matlab.

To calculate the wear rate(K), using Archard wear rate, which is calculated as the total volume worn, V (in mm^3), divided by the product of applied normal load, F_n (in N), andsliding distance, d (in m), and the equation shows below:

$$K\left[\frac{mm^3}{Nm}\right] = \frac{V[mm^3]}{F_n[N] \times d[m]} \quad (1)$$

In practicality, the 3D height profile of the wear scar was measured using the SWLI. Fifty-four 2D height map cross sections are acquired along each wear scar to measure cross-sectional area of the wear scar. The Archard wear rate can then be calculated from these experimentally measured cross-sectional areas by Equation (2)[59]:

$$K\left[\frac{mm^3}{Nm}\right] = \frac{A[mm^2]}{F_n[N] \times C} \times 10^3 \left[\frac{mm}{m}\right] \quad (2)$$

where A is the measured cross-section area of wear scar (in mm2) and C is the number of reciprocating sliding cycles (1 cycle is one forward and one reverse stroke).

2.4.3 Scanning wear scar

When using SWLI to scan the wear scar, a Pi micos rotary stage was introduced. Because we want to figure out tribological properties on the different crystal direction of GaN. Therefore, we use SWLI to scan and take pictures on every 15 degrees of the GaN. After we got all the data for the wear scars, then we can use another Matlab code to analyses them and get a relatively accurate math matrix of the areas of the scars.

Figure 7: Pi micos rotary stage, controlled by the software to get a precise position

2.5 Method to measure the area of wear scars

Using a Matlab code, choose 3 scan parts for each specific direction of wear scars. Then there are 3 basic steps to calculate the area for the wear scar, we choose the experiments under the 0.5mps, 0.3N to look:

First is to scan the scar like figure 8.

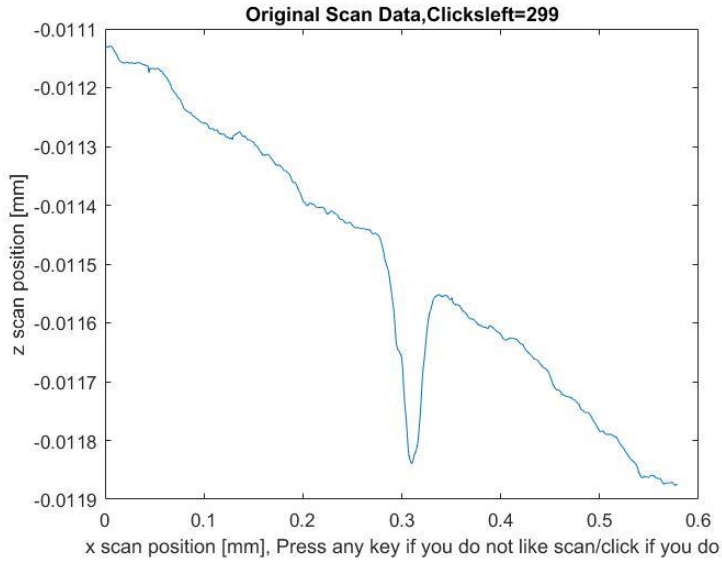

Figure 8: the scan for tilt profile

Then click the 4 points even in the tilt profile to simulate the scan line in matlab code to level it like figure 9.

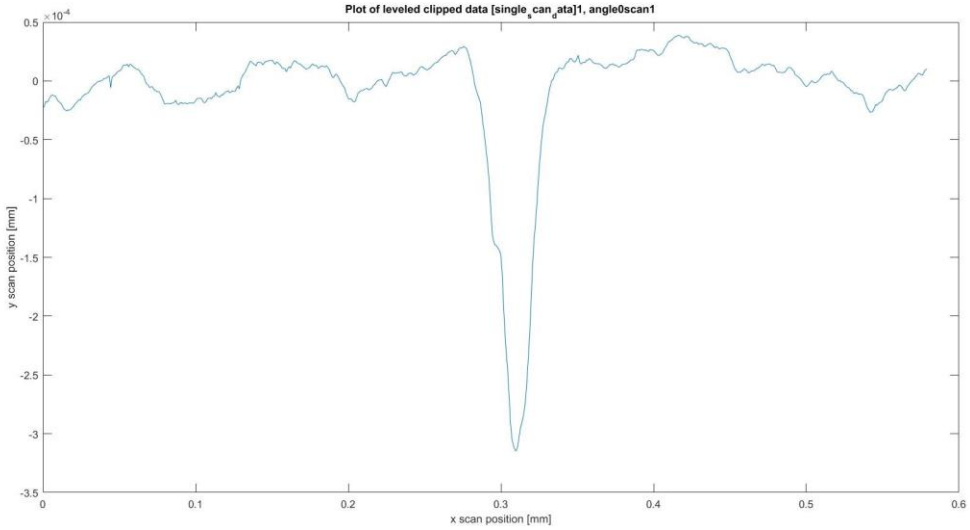

Figure 9:the scan for leveled profile

And the final step is to select the wear area to make a calculation by Matlab, and the red region in figure 10 is the area we need to integrate.

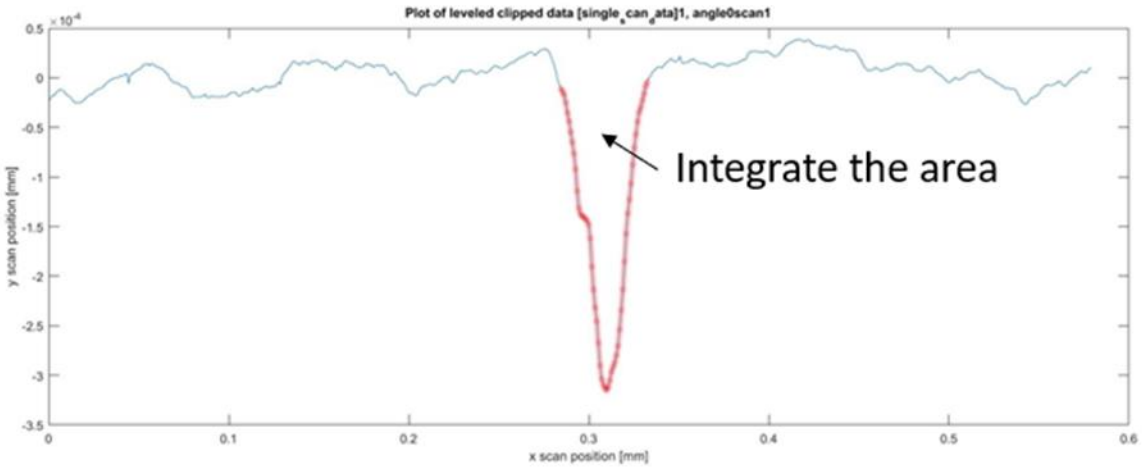

Figure 10:the selected region to do numerical integrate

2.6 Uncertainty

There are several errors in the experiments:

First, the normal force is not stable in these high speed, the probe tilts up and down when touch the spinning sample, that caused some errors. Although, most of the deviations can be controlled in 30(in mN), some of the errors even surpass 100 (in mN), which influenced the data accuracy.

Secondly, when scanning the wear scars, the SWLI has errors both on the width and height of the real data of scars, and these errors may ample when changing the degrees of the sample. Moreover, when deal with the data of these profiles, the calculation by Matlab code also produce some errors.

Also, some errors produced by machine and assemble procedures, some uncontrolled artificial mistakes are cannot be avoided.

3.Results and Discussion

3.1 First group of experiments

3.1.1Profile of wear scars

Using SWLI, we can get scan pictures of the 4 different conditions, choose the 0 degree to refer to the scar profiles, like the figures below:

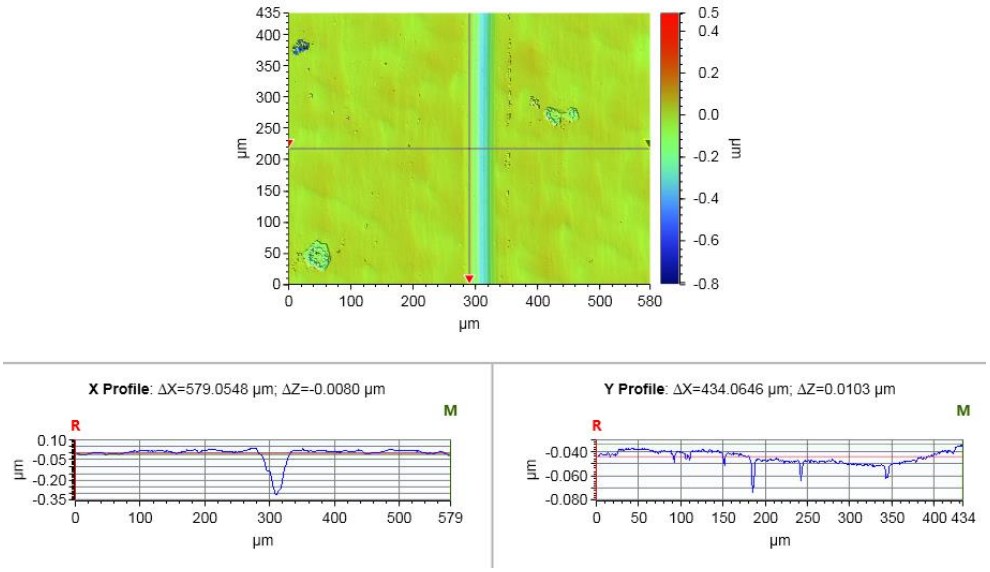

Figure 11: The profile of wear scar in 0 degree for the experiment in 0.5m/s and 0.3N

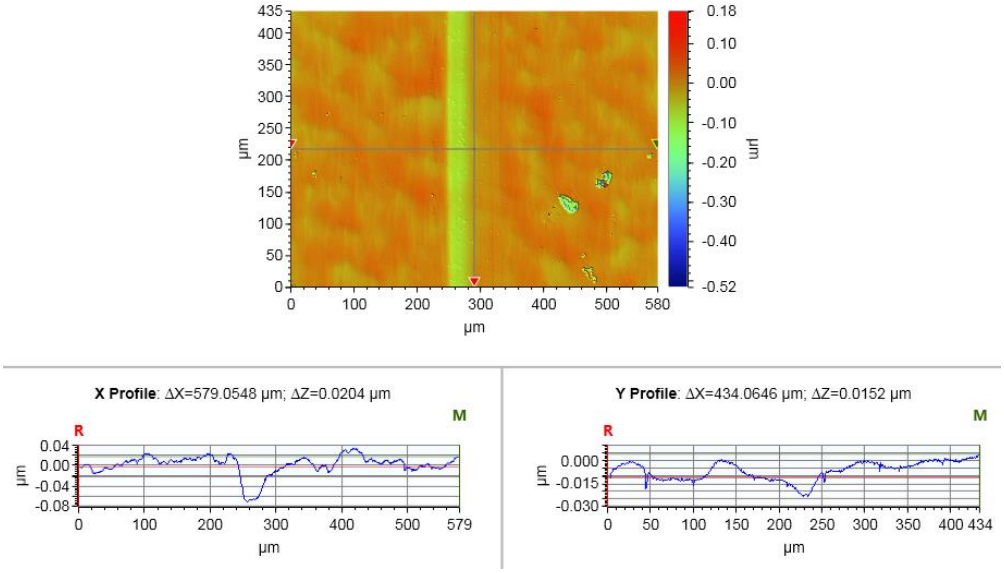

Figure 12: The profile of wear scar in 0 degree for the experiment in 0.5m/s and 0.9N

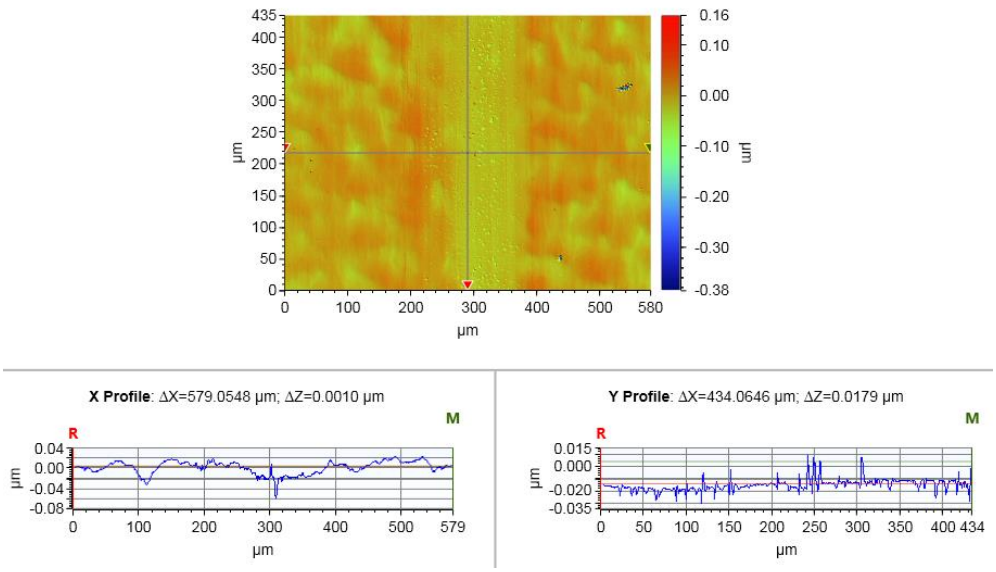

Figure 13: The profile of wear scar in 0 degree for the experiment in 1m/s and 0.3N

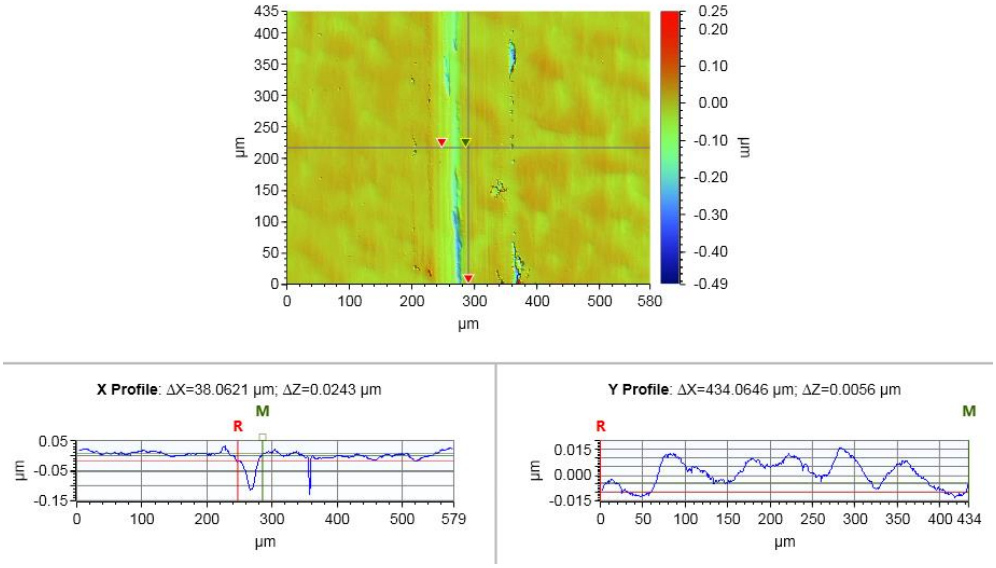

Figure 14: The profile of wear scar in 0 degree for the experiment in 1m/s and 0.9N

From these figures we can see that, there is no wear scar on the third groups of experiments, the reason is probably the ruby ball is off the probe when sliding on the sample. And we can also get some information about the depth and width of the scar, for example, we can see that, width of the scar is approximately 36.2476µm, the depth is around 0.02µm in the figure 14. Moreover, for the 0 degree, we can see the surface plots for each experiment, and in the surface plot figure 17, we can see clearer that, the surface of the sample does not exist wear scars.

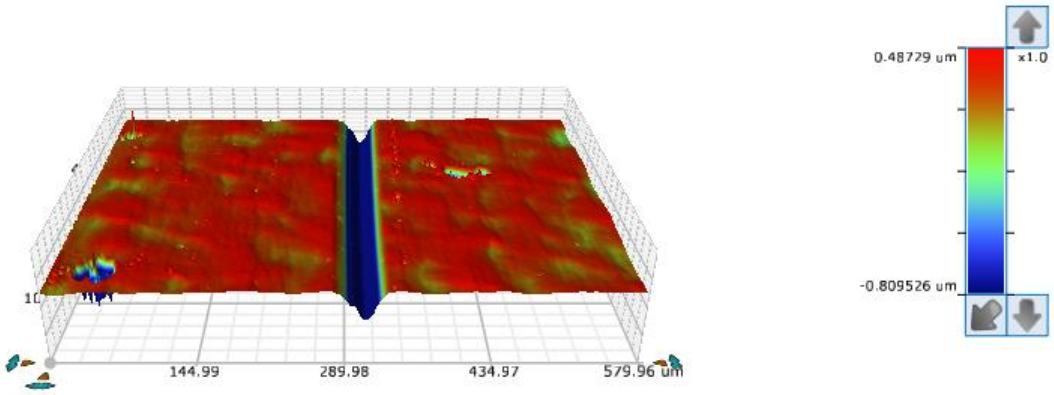

Figure 15: Surface plot for the experiment in 0.5m/s and 0.3N (Note: there are none linear in Z color scale)

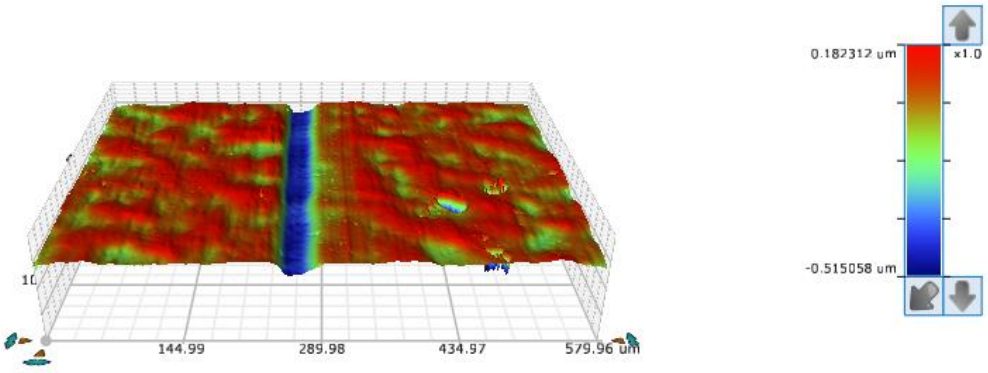

Figure 16: Surface plot for the experiment in 0.5m/s and 0.9N (Note: there are none linear in Z color scale)

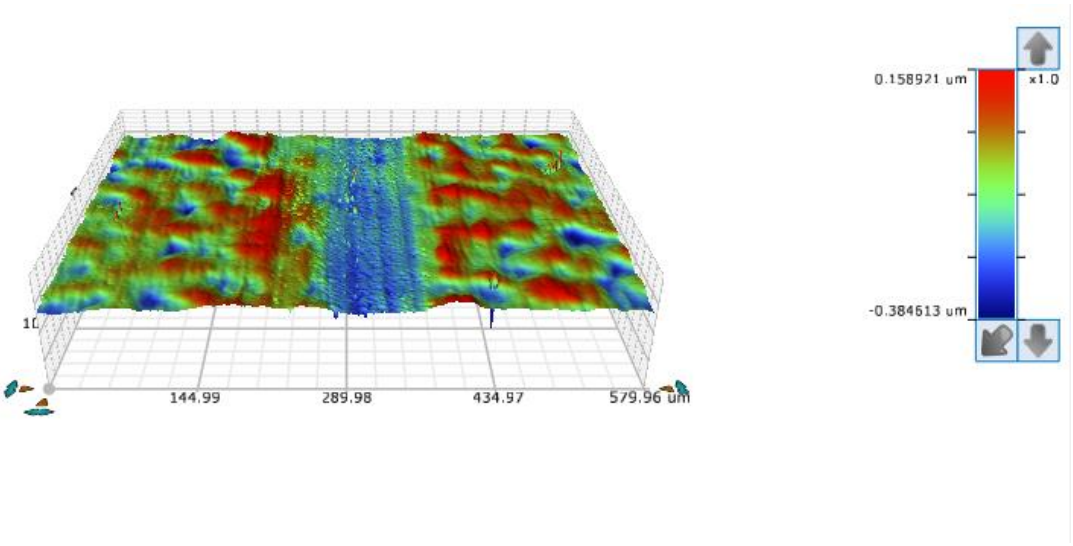

Figure 17: Surface plot for the experiment in 1m/s and 0.3N (Note: there are none linear in Z color scale)

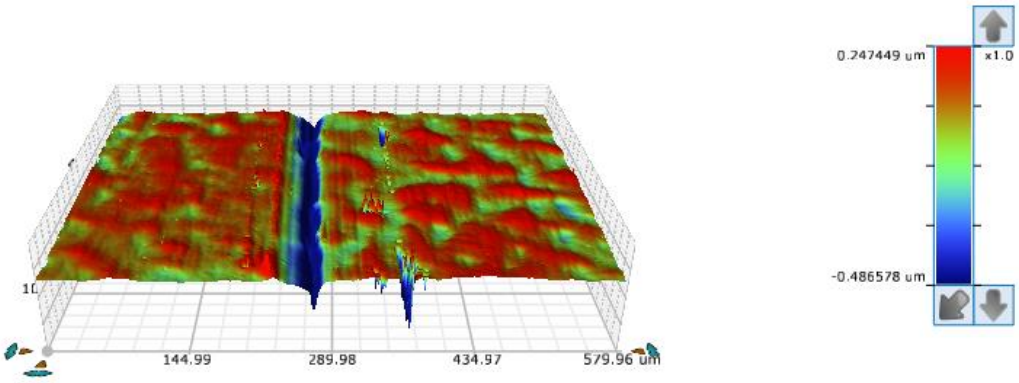

Figure 18: Surface plot for the experiment in 1m/s and 0.9N (Note: there are none linear in Z color scale)

3.1.2 Coefficient of friction

Recorded by the Matlab data, we can simply invoke the average normal forces, friction, and coefficient of friction for each experiment, shows in the figures below. And from the average data for each circle of each experiment, we can calculate the numerical mean values of the COF, the COF is 0.389733 with 0.3N, 0.5m/s; 0.31119 with 0.9N, 0.5m/s; and 0.313259 with 0.9N, 1m/s. And for the failed experiment for the 1m/s, 0.9N, we can see the abnormal friction and

COF, since the ruby ball off when it still running, and there is no wear scar on that. Therefore, according to the three effective COF, we can see the COF of GaN is stable on the high speed, for the low loads, the bigger COF is probably caused by the initial unstable friction, we can see it from figure 19, the middle graph. Then if we average the three number, we can get the COF is 0.338061, approximately equals to the 0.35 in low humidity environment[55].

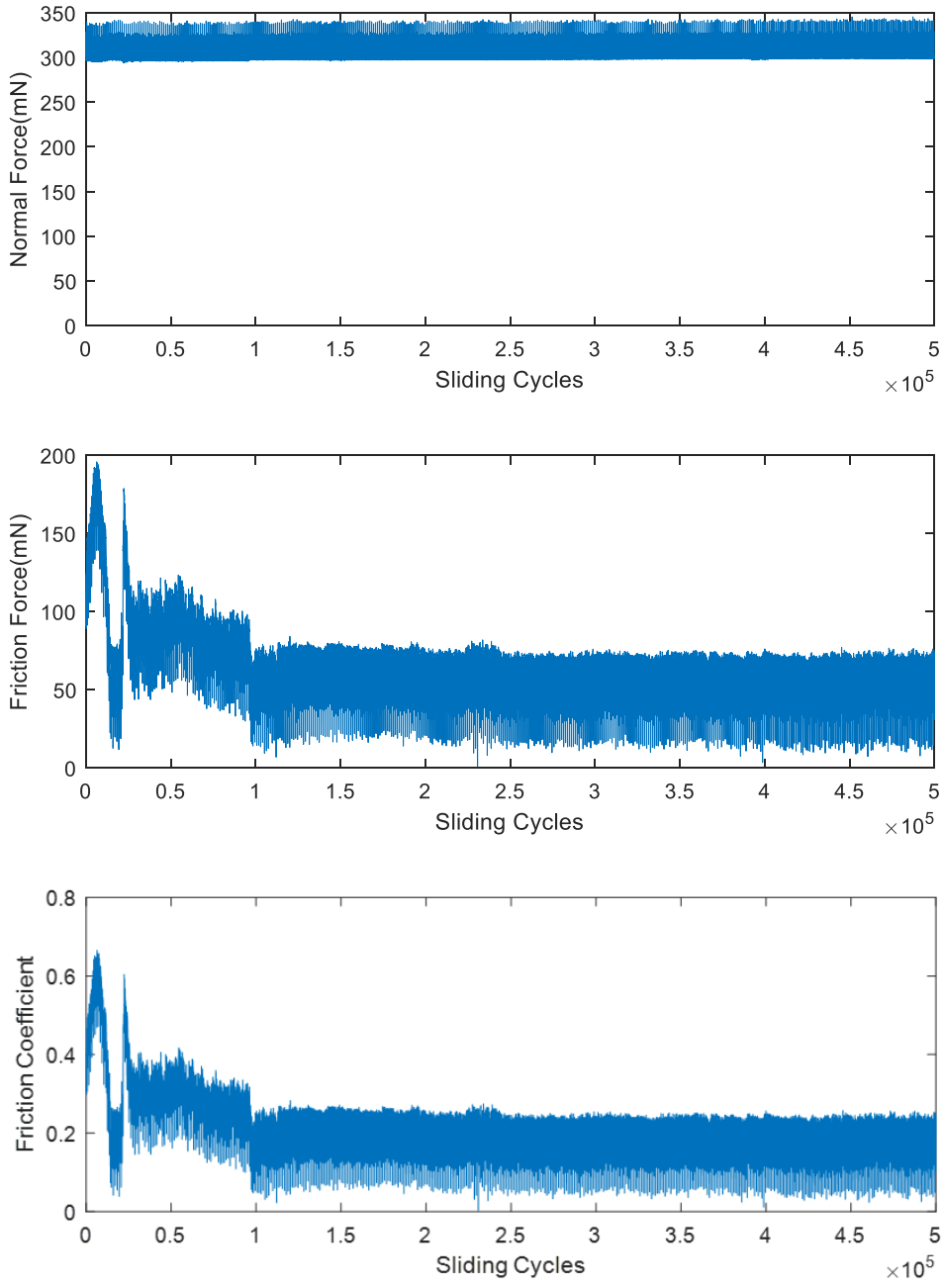

Figure 19: COF, Normal force, Friction for the experiment in 0.5m/s and 0.3N (figures from top to bottom are: normal force, friction, COF vs sliding cycles)

From the figure 19, we can see the normal force is relatively stable at 300mN, the friction has an initial unstable stage, probably caused by the rotary. And from the bottom picture, we can see the COF is finally stable around 0.2.

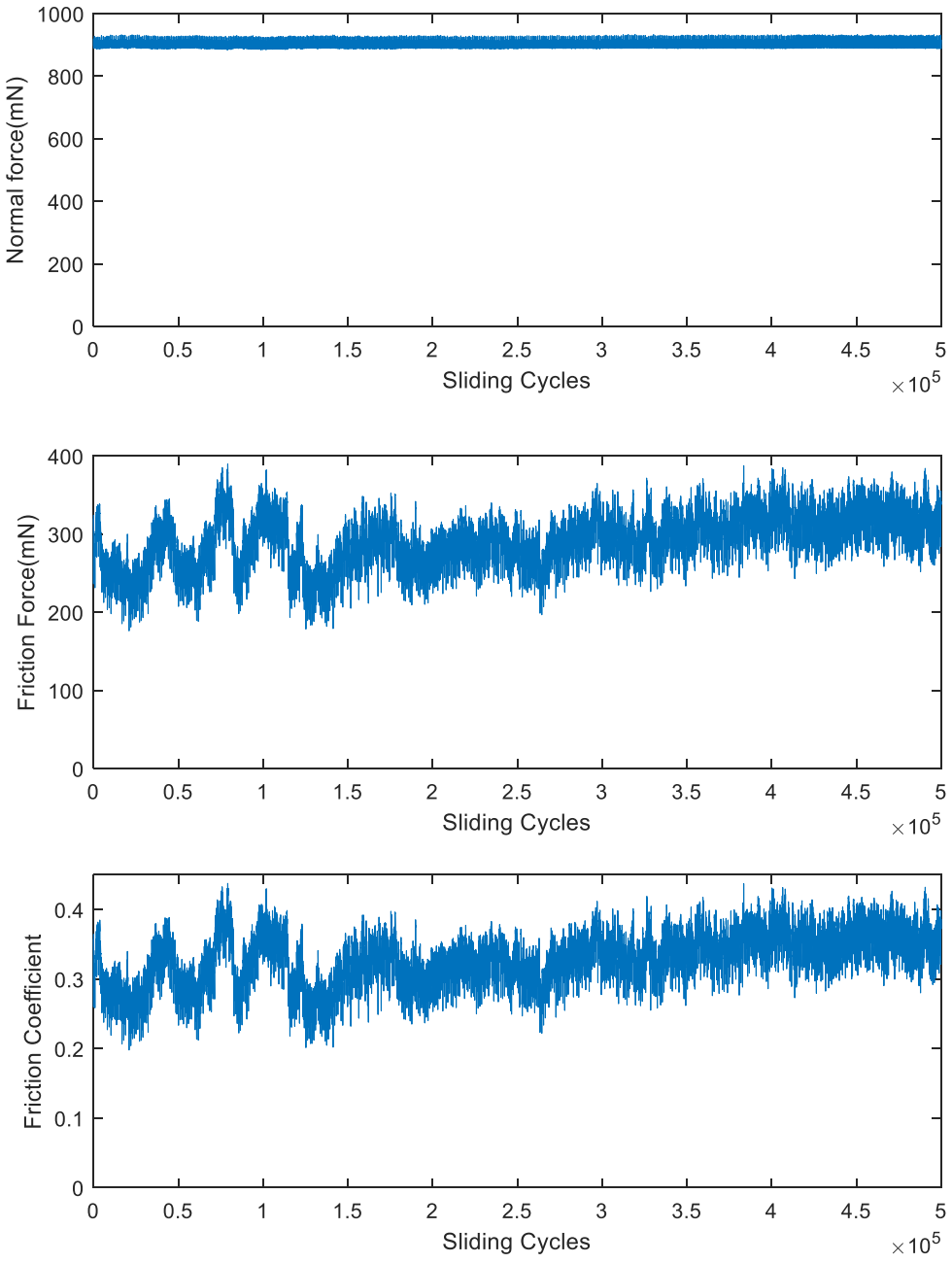

Figure 20: COF, Normal force, Friction for the experiment in 0.5m/s and 0.9N (figures from top to bottom are: normal force, friction, COF vs sliding cycles)

From the figure 20, we can see the normal force is relatively stable at 900mN, the friction is not very stable stage, probably caused by the high loads. And from the bottom picture, we can see the COF is finally stable around 0.35.

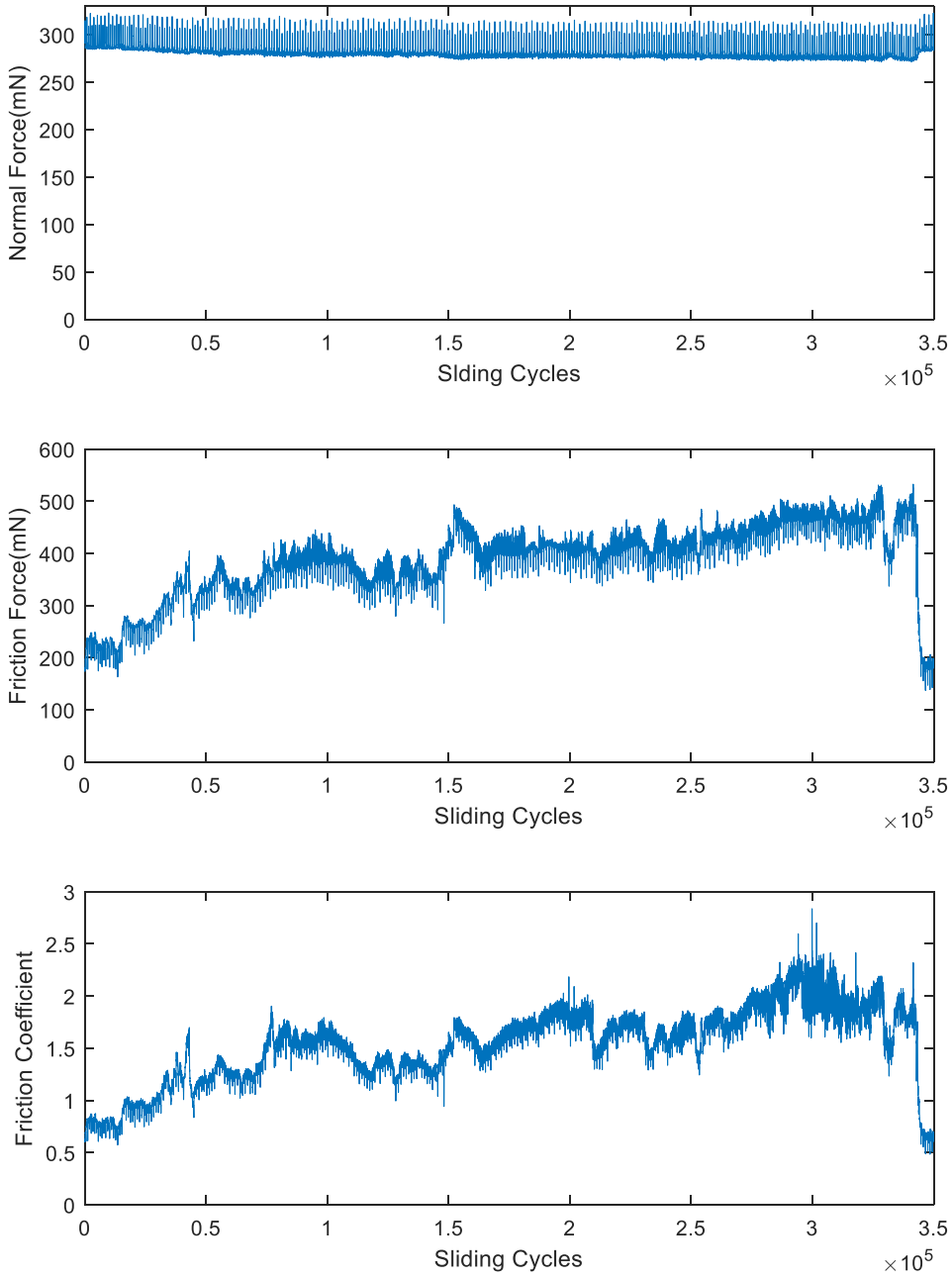

Figure 21: COF, Normal force, Friction for the experiment in 1m/s and 0.3N (figures from top to bottom are: normal force, friction, COF vs sliding cycles)

From the figure 21, we can see the normal force is relatively stable at 300mN, the is unstable, probably caused by the high frequency tilts and dry environments. And from the bottom picture, we can see the COF is not stable at all, the flat is probably tilt when sliding.

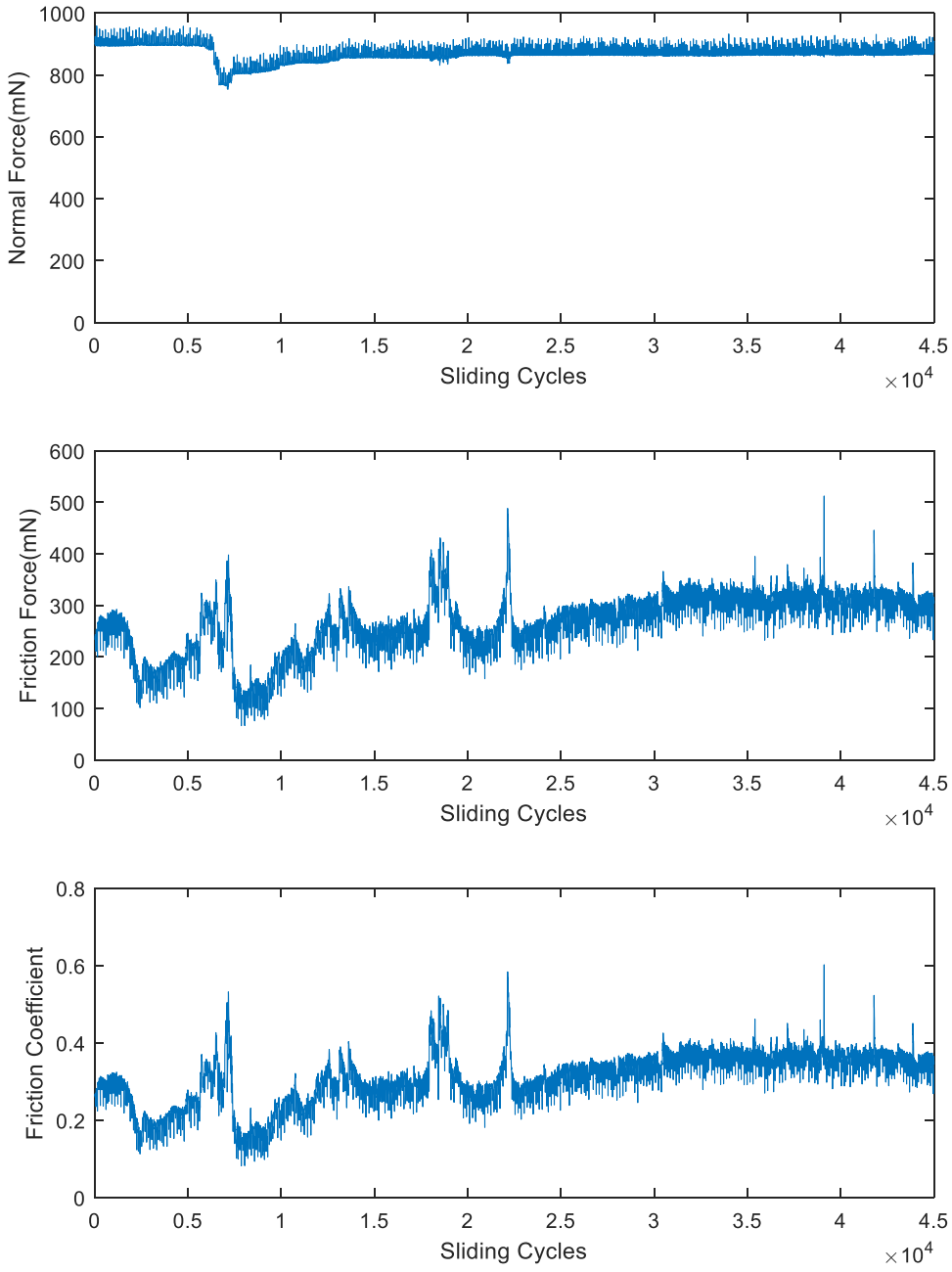

Figure 22: COF, Normal force, Friction for the experiment in 1m/s and 0.9N (figures from top to bottom are: normal force, friction, COF vs sliding cycles)

From the figure 22, we can see the normal force is more stable after 10 thousand cycles, the friction is also unstable relatively. And from the bottom picture, we can see the COF is also unstable but approximately around 0.3. This test is probably influenced by the high speeds and high loads

To make better comparison, we compare the COF in different normal forces and different sliding speeds. Unlike the humidity, from figure 24, we can see the high speed is not a controlling factor for COF, also since the high speed in sliding and angular, the contact region is not stable. The plate may be tilting, and the probe may vibrate. Both these experiment errors are make the COF of the high speed in a relatively high fluctuation.

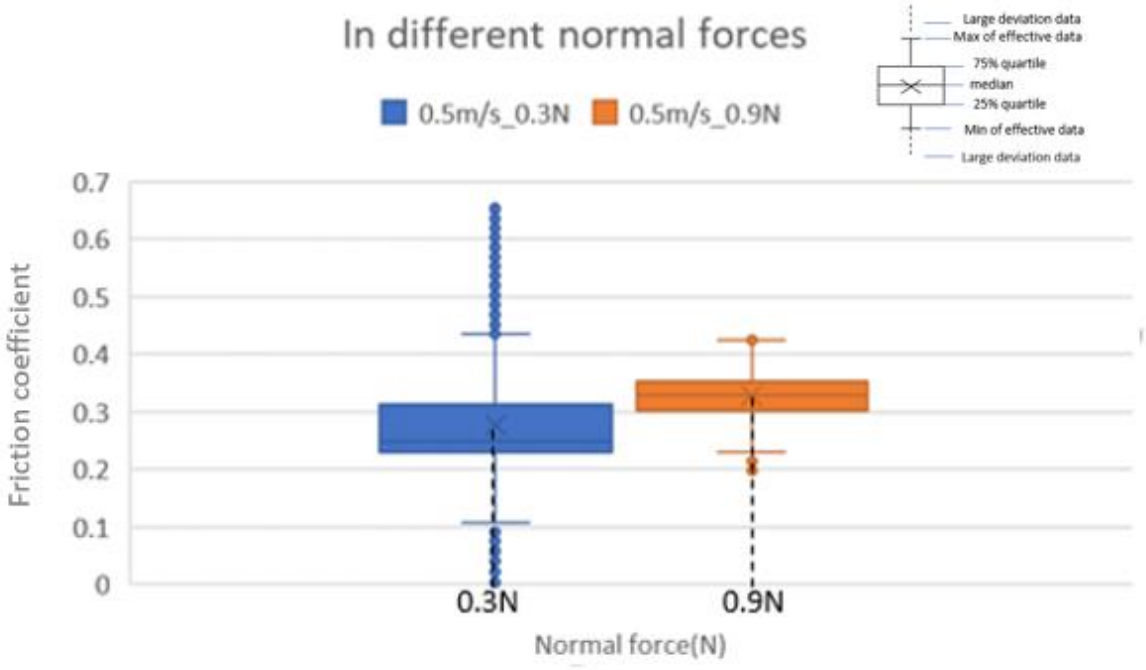

Figure 23:COF in different normal forces. (Note: since the plate is tilting when sliding, there are several data has a huge deviation)

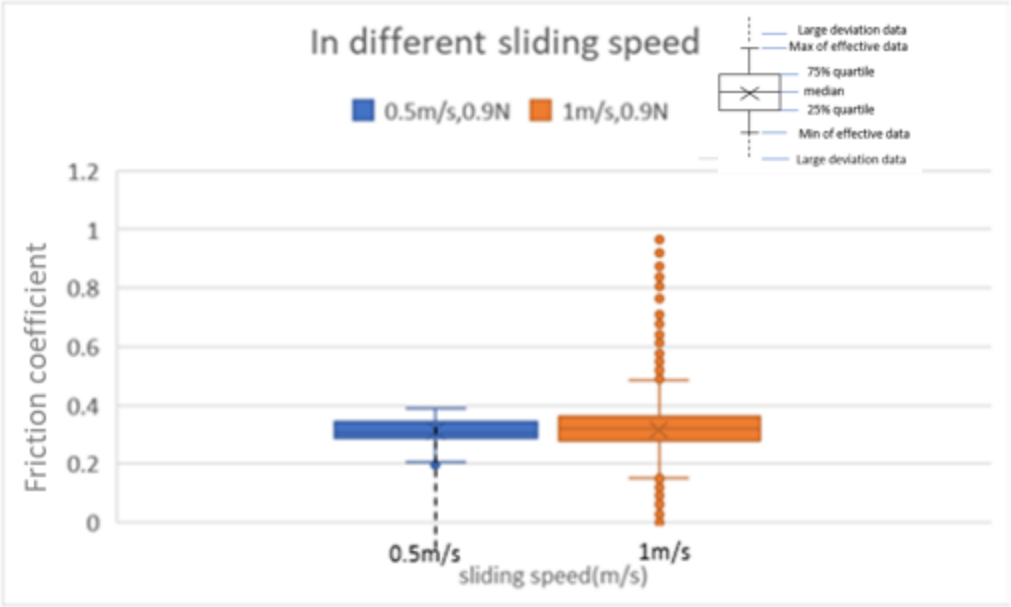

Figure 24:COF in different sliding speeds. (Note: since the plate is tilting when sliding, there are several data has a huge deviation)

3.1.3Wear Rate

From the below figures, wear rates in different angles, we can see that, in 0.5m/s, 0.3N, the wear rate reaches approximately 2×10^{-7} to $3 \times 10^{-7} \mathrm{mm}^3/Nm$, and it shows around a 60 -degree period of the wear rate which accord with the research by Guosong Zeng et. al., which observed a 60° periodicity of wear rate[56]. And according to the data the highest wear rate for each period appears on the 0, 60, 120, 180, 240, and 300 degrees, and the lowest wear rate in the period appears on the 15,90,150,210,255,330 degrees. Still, we should notice that the highest of the wear rate in whole angles is in 180-degree, arrives on approximately $2.8 \times 10^{-7} \mathrm{mm}^3/Nm$. The lowest of the wear rate is in 90-degree, approximately $1.9 \times 10^{-7} \mathrm{mm}^3/Nm$. These outcomes also coincide with the research mentioned above shows that, the highest wear rate appears in the $< 1\bar{2}10 >$crystal direction of the GaN, and the lowest wear rate appears in the$< 1\bar{1}00 >$direction.

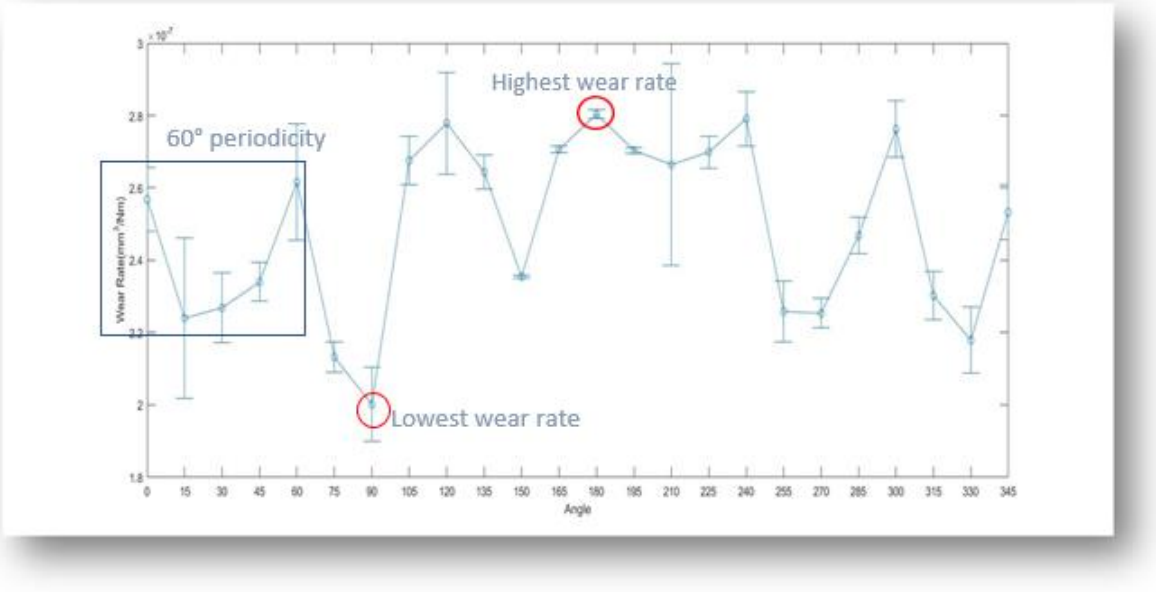

Figure 25: Wear rates in different angles at the experiment under the 0.5m/s, 0.3N

In a similar way, from the figure 26, we can get the wear rate reaches approximately 2×10^{-8} to $4 \times 10^{-8}\text{mm}^3/Nm$, and it also shows around a 60-degree period. The highest of the wear rate in whole angles is in 240-degree, arrives on approximately $4.3 \times 10^{-8}\text{mm}^3/Nm$. The lowest of the wear rate is in 330-degree, approximately $1.8 \times 10^{-8}\text{mm}^3/Nm$. The highest wear rate for each period appears on the 0, 60, 120, 180, 240, and 300 degrees, and the lowest wear rate in the period appears on the 30,75,135,195,270,330 degrees.

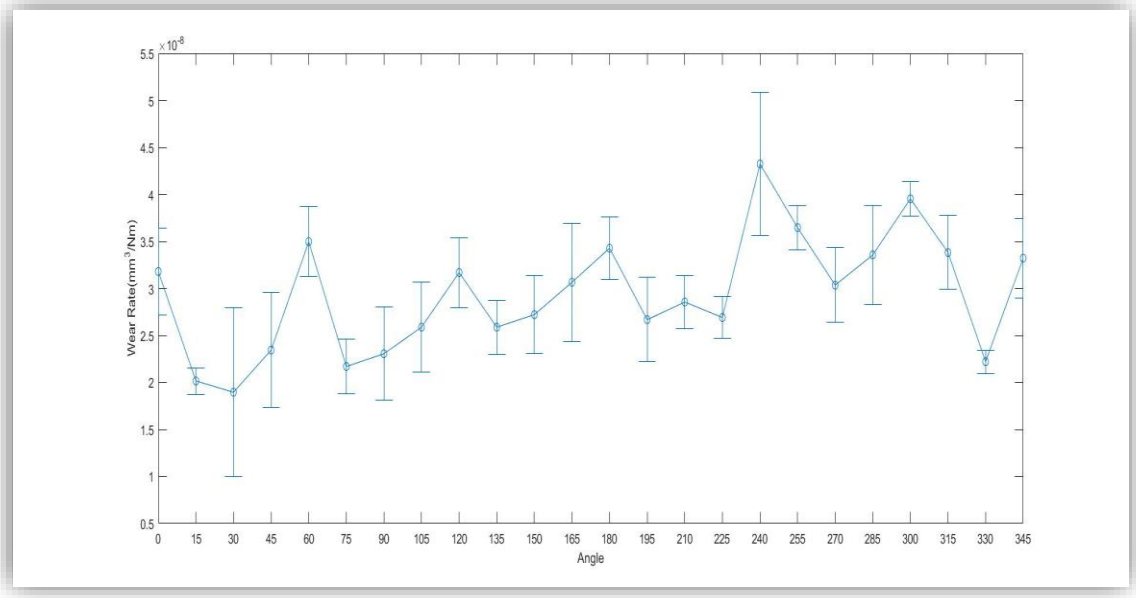

Figure 26: Wear rates in different angles at the experiment under the 0.5m/s, 0.9N

And the figure 27 shows the wear rate reaches approximately0.5×10^{-8} to $4 \times 10^{-8}\text{mm}^3/Nm$, and it also shows around a 60-degree period. The highest of the wear rate in whole angles is in 180-degree, arrives on approximately $4 \times 10^{-8}\text{mm}^3/Nm$. The lowest of the wear rate is in 135-degree, approximately $0.6 \times 10^{-8}\text{mm}^3/Nm$. The highest wear rate for each period appears on the 0, 60, 105,180, 240, and 285 degrees, and the lowest wear rate in the period appears on the 45,90,135,210,270,330 degrees. These data have big errors because the probe tilted lots under the high speed and high loads.

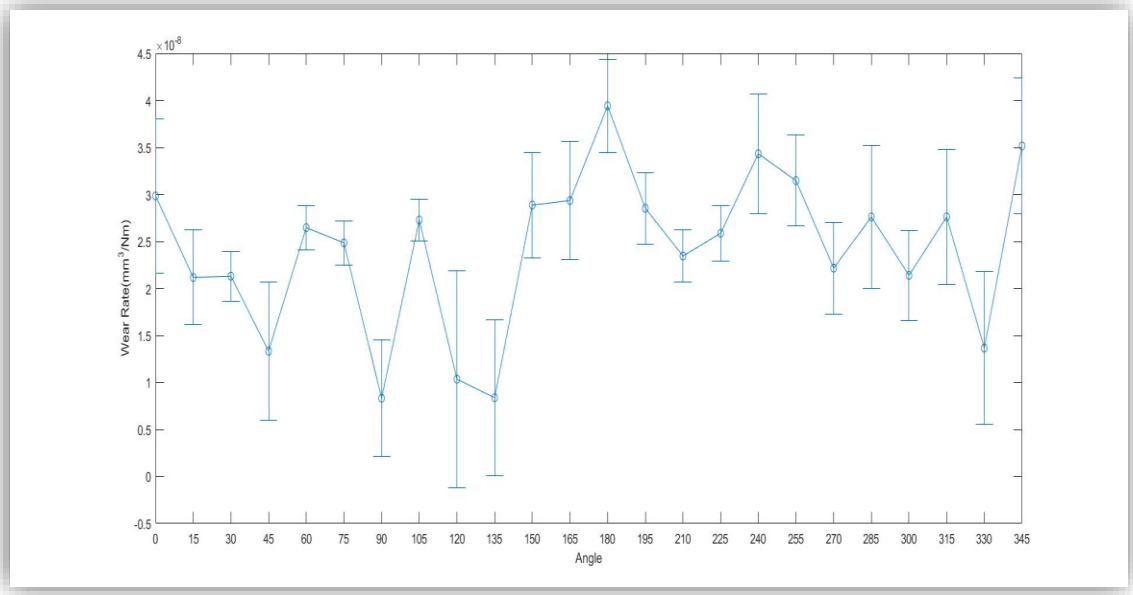

Figure 27: Wear rates in different angles at the experiment under the 1m/s, 0.9N

Beside the interesting information about the relationship between the crystal direction and wear rates. We can still compare different forces in same degree and same sliding speeds. In the figure 28, we can clear observe that wear rate is lower when force is higher. And it changes a magnitude order. After average both wear rates in different normal forces, we can approximately get $2.49\times10^{-7}\text{mm}^3/\text{Nm}$ in the 0.3N, and 2.92×10^{-8} mm^3/Nm, which means wear rate $\overline{\text{K}}_{0.5\text{mps},0.3\text{N}} \approx 8.5\overline{\text{K}}_{0.5\text{mps},0.9\text{N}}$. From the equation Archard wear rate, we can easily get that the wear rate is inversely proportional relationship to the normal force. Theoretically, if we assume the normal forces are stable, then, we can get the normal force $\overline{\text{Fn}}_{0.5\text{mps},0.3\text{N}} = \frac{1}{3}\overline{\text{Fn}}_{0.5\text{mps},0.9\text{N}}$, Therefore, we can get the area of the scar $\overline{\text{A}}_{0.5\text{mps},0.3\text{N}} \approx 2.8\,\overline{\text{A}}_{0.5\text{mps},0.9\text{N}}$, that means the material losses under the 0.3N is larger than it under the 0.9N. My hypothesis for that results is that first the normal force for 0.9N is not stable, especially after finishing a big number of circles, in some direction the normal force is a way larger than the 0.9N, therefore, it calculates much smaller. The second probably reason is that the really low relatively humidity, according the Wear rate of GaN tested under different environments we formal did in our lab, the dry air will lower the wear rate[57].

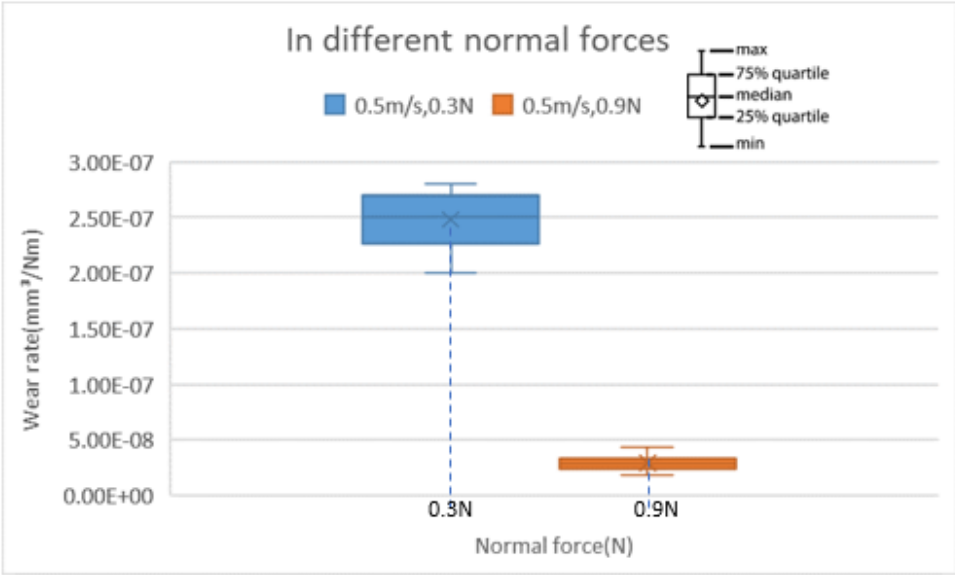

Figure 28: under the 0.5m/s sliding speed, wear rates in different forces

And compare different sliding speeds in same degree and same forces, we can get the figure 29, and we can see, the faster the sliding speed, the lower the wear rates. First of all, because of the low humidity, the magnitude order of wear rate is from 10^{-8} to 10^{-7} mm^3/Nm[57], and in the same force, there is no remarkable change in the Archard's law. Under the 0.9N, we get the average of wear rate for 0.5m/s is 2.92×10^{-8} mm^3/Nm, and 2.39×10^{-8} mm^3/Nm. Although, the change rate is small, we can still find that, high speed will influence the wear rate of GaN.

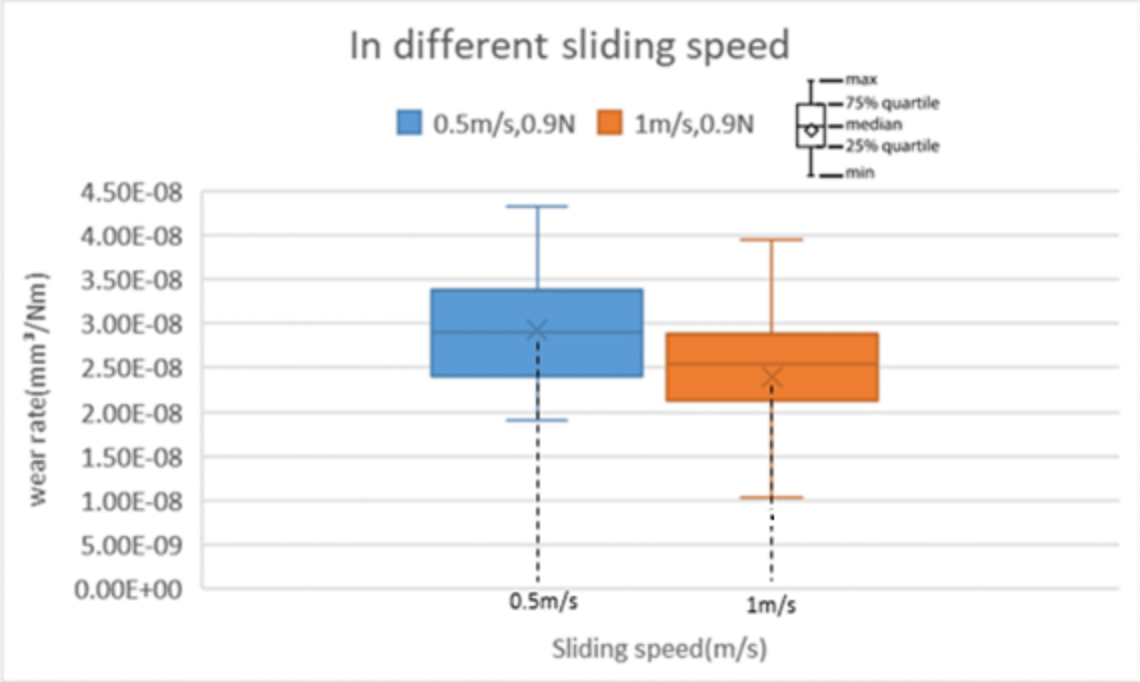

Figure 29: under the 0.9 N normal force, wear rates in different sliding speeds

And all the average wear rates in the three groups of experiment in different angles shows in the table 4.

Angles	Wear rate (mm^3/Nm) 0.5m/s,0.3N	Wear rate (mm^3/Nm) 0.5m/s,0.9N	Wear rate (mm^3/Nm) 1m/s,0.9N
0	2.57E-07	3.18E-08	2.98E-08
15	2.24E-07	2.02E-08	2.12E-08
30	2.27E-07	1.9E-08	2.13E-08
45	2.34E-07	2.34E-08	1.33E-08
60	2.62E-07	3.5E-08	2.65E-08
75	2.13E-07	2.17E-08	2.48E-08
90	2E-07	2.31E-08	8.32E-09
105	2.68E-07	2.59E-08	2.73E-08
120	2.78E-07	3.17E-08	1.03E-08
135	2.64E-07	2.59E-08	8.38E-09
150	2.35E-07	2.72E-08	2.89E-08
165	2.71E-07	3.07E-08	2.93E-08
180	2.8E-07	3.43E-08	3.94E-08
195	2.7E-07	2.67E-08	2.85E-08
210	2.66E-07	2.86E-08	2.35E-08
225	2.7E-07	2.69E-08	2.59E-08
240	2.79E-07	4.32E-08	3.43E-08

255	2.26E-07	3.65E-08	3.15E-08
270	2.25E-07	3.04E-08	2.22E-08
285	2.47E-07	3.36E-08	2.76E-08
300	2.76E-07	3.95E-08	2.14E-08
315	2.3E-07	3.38E-08	2.76E-08
330	2.18E-07	2.22E-08	1.37E-08
345	2.53E-07	3.32E-08	3.52E-08

Table 3: Wear rates in different angles

3.1.4 Scanning electron microscope(SEM) for wear scars

Worn surface morphology was analyzed by scanning electron microscopy (SEM, ZEISS 1550) to compare the wear modes for different environments. The inhomogeneity of the surface states was visualized and confirmed with low voltage scanning electron microscopy (LVSEM). Upward band bending will build up an electrical field pointing from the bulk to the surface[58]. Applying 5 different voltages, 0.5kV, 1kV, 2.5kV, 5kV, 10kV, to scan the profile of the scars. We use 0.9N,0.1m/s as an example in Fig. 30. When applying a low accelerating voltage, this electrical field will depress the emission of secondary electrons from the top surface and give rise to a secondary electron (SE) contrast (i.e., dark area in micrograph, see Fig. 30a). However, when the accelerating voltage is above a critical value, 5 kV, the SE become lower. We can hypothesis that there is a band bending through the sliding tests.

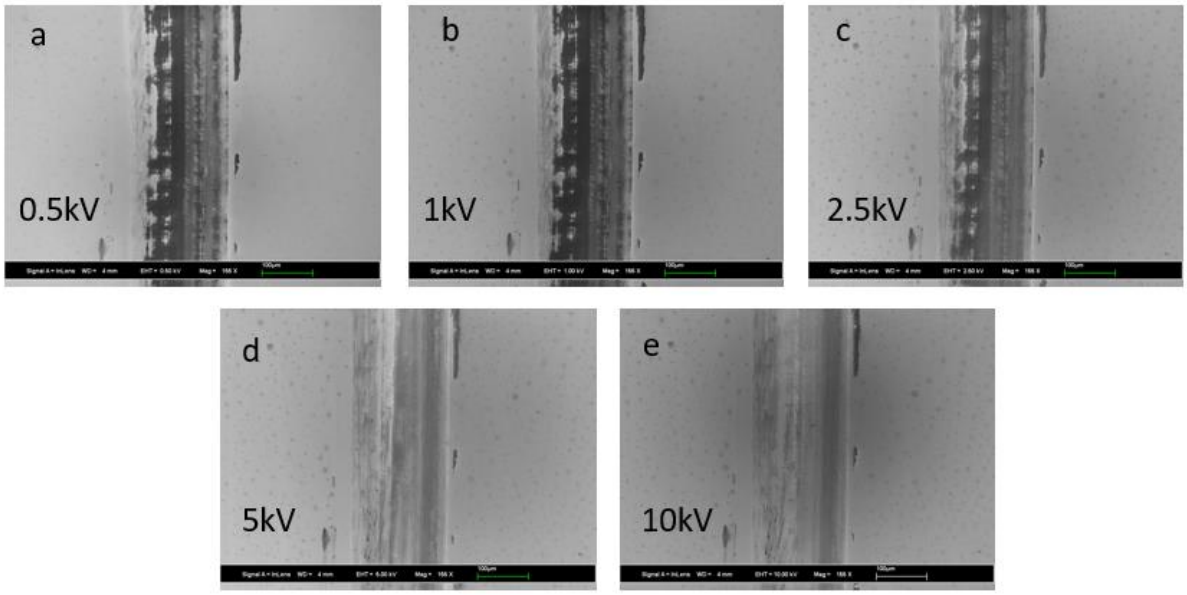

Figure 30:Visualization of the inhomogeneous shear-modified surface by low voltage SEM. (a) 0.5 kV; (b) 1 kV; (c) 2.5 kV; (d) 5 kV; (e) 10 kV

We can also compare the different parameters of wear scars in same voltages, we use the 1kV as the specific one to analysis the electrical field. The figure 31 shows different normal forces, and the 32 shows different sliding speeds. In figure 31, we can see that, the band states are contrast, which indicates the procedure of tribodoping may in different procedures. Also, we can see the higher the loads, the darker the region of the band states, which indicates different loads influence the band bending. And we hypothesis that, the higher the loads, the more intensity of the band bending. In the similar way, in figure 32 we can see different sliding speeds influence the band bending. And we hypothesis that, the higher the speeds, the more intensity of the band bending.

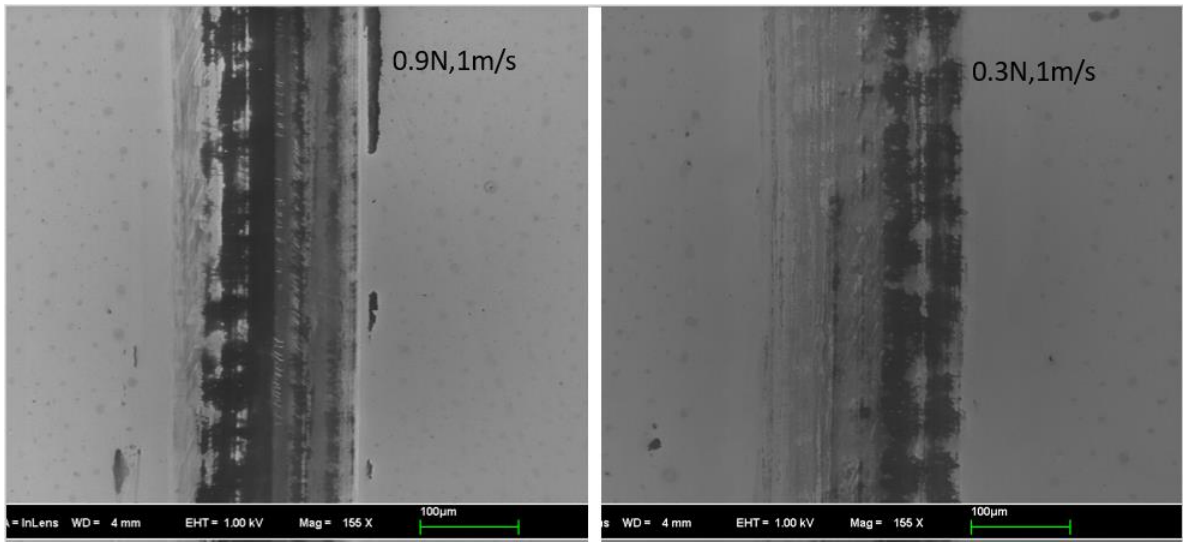

Figure 31:Visualization of the inhomogeneous shear-modified surface by 1kV SEM in different normal forces, left is in 0.9N, right is in 0.3N

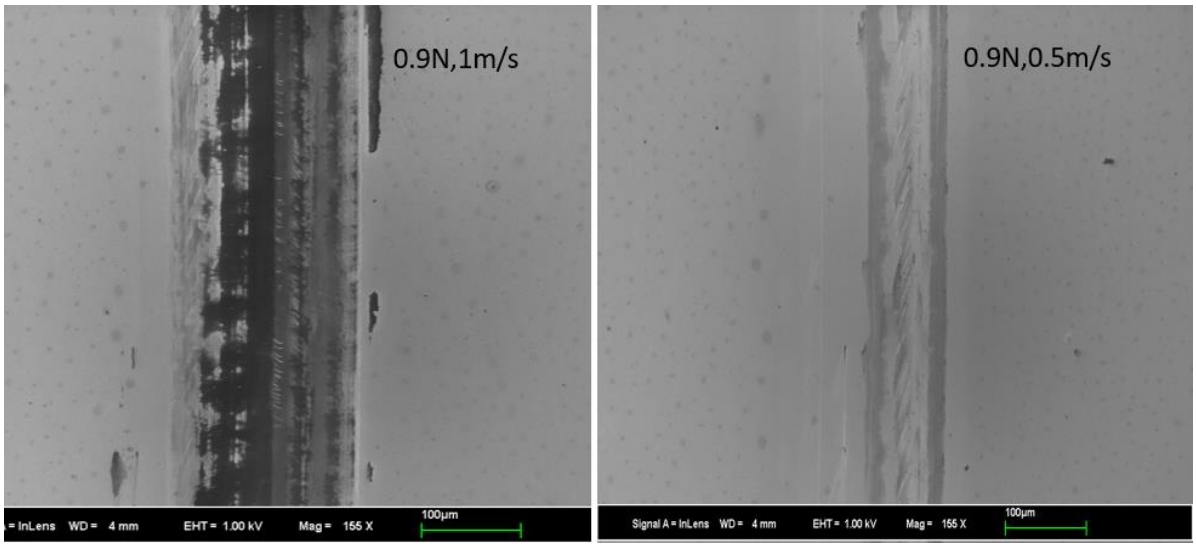

Figure 32:Visualization of the inhomogeneous shear-modified surface by 1kV SEM in different sliding speeds, left is in 1m/s, right is in 0.5m/s.

3.2 Second group of experiments

3.2.1 Coefficient of friction

Since we already observe the periodical wear rates of GaN. In second experiments, we are focus on how the different sliding speeds influence the tribological properties of the GaN. In figure 33, we can see the different COF in different sliding speeds in 0.3N. And in figure 34, we can see the different COF in different sliding speeds in 0.9N.

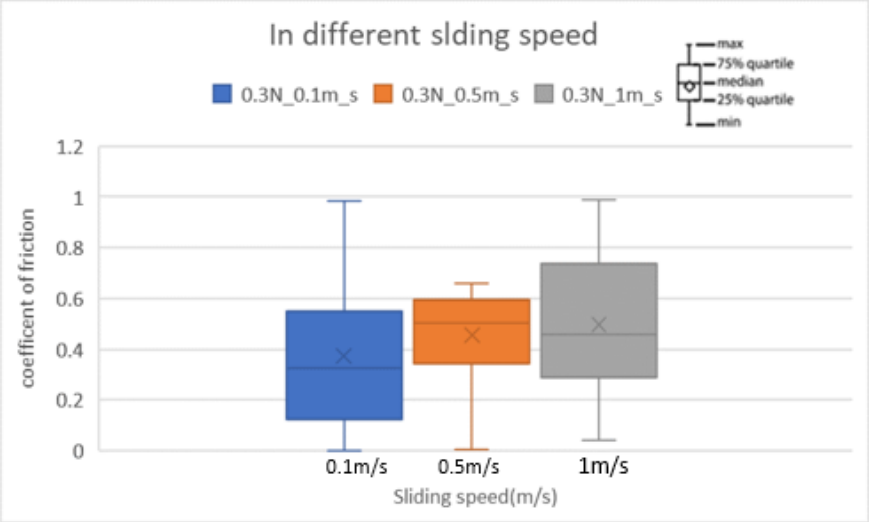

Figure 33:COF in different sliding speeds under 0.3N

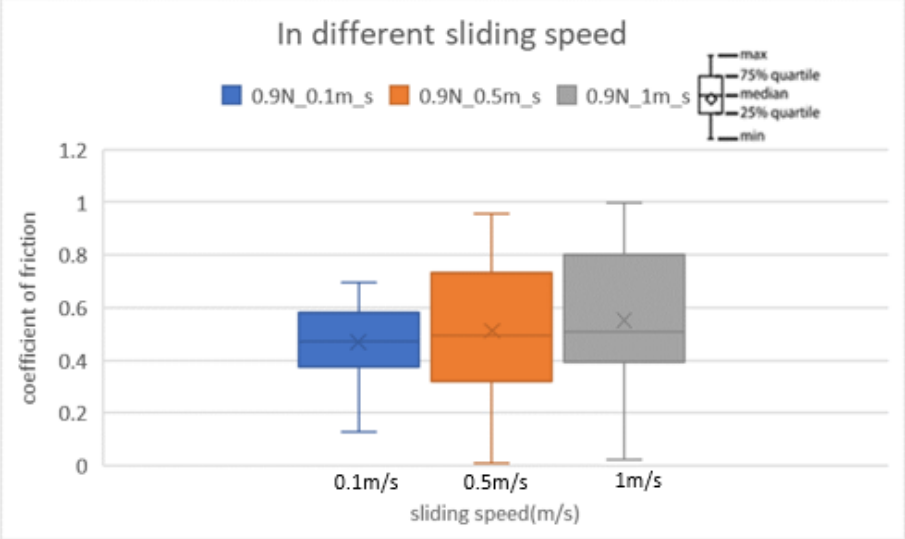

Figure 34:COF in different sliding speeds under 0.9N

And if we calculate the numerical average number of COF in different controlling parameters, we can get details in table 5. We can conclude that, the COF is higher in high loads and high speeds.

COF	0.3N	0.9N
0.1m/s	0.373729	0.468343
0.5m/s	0.45643	0.512917
1m/s	0.496895	0.550821

Table 4: Average number of COF in different conditions

3.2.2 Wear Rate

Since we already observed the periodical wear rate, around every 60 degrees of the crystal direction, of GaN. In the second group of experiments, we just scanned the wear scars end in 90 degrees. And the figure 35 shows the detail of every wear rates versus degrees, also the crystal direction of the GaN in different sliding speeds under the 0.3N. In the similar way, the figure 36 shows that under the 0.9N. From these pictures, we can take a glance at how the wear rates change from 0-degree to 90-degree.

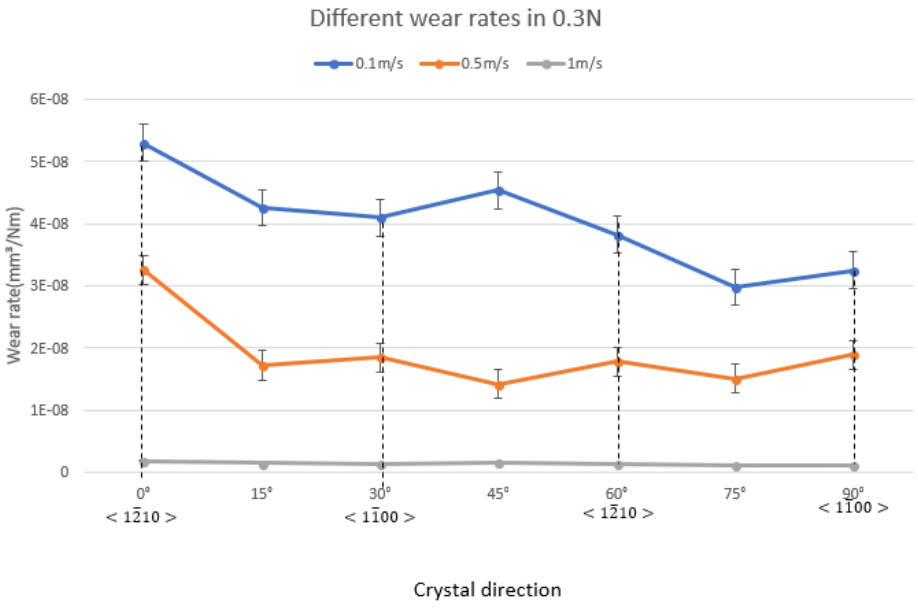

Figure 35: Wear rates in different degrees, with three different sliding speeds under the 0.3N

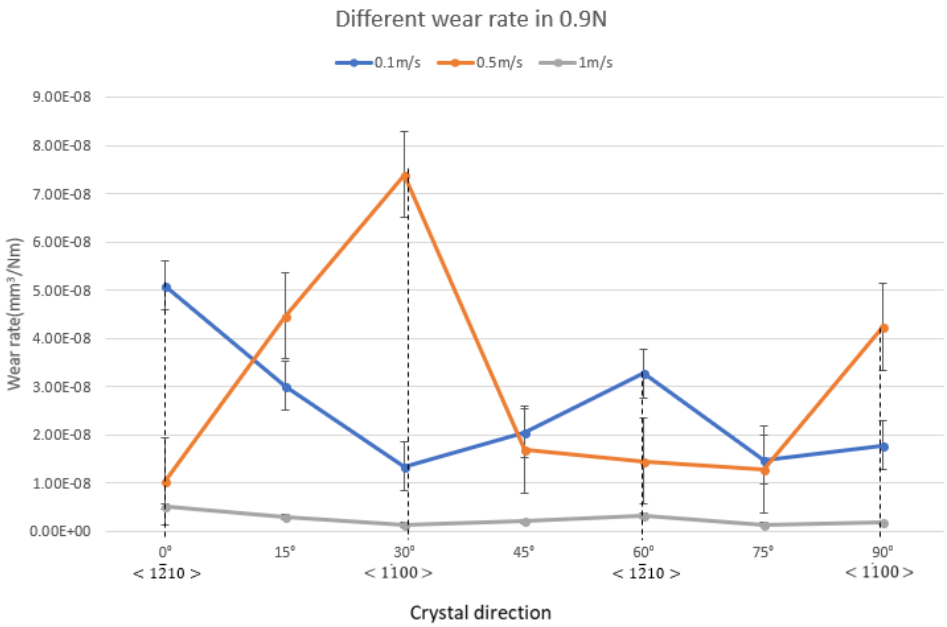

Figure 36: Wear rates in different degrees, with three different sliding speeds under the 0.9N

To calculate the wear rates and show more details, we can get information about the numerical average number of wear rates in each experiment in table 6.

Degree	0.1m/s,0.3N Wear rate(mm^3/Nm) ($x10^{-8}$)	0.5m/s,0.3N Wear rate(mm^3/Nm) ($x10^{-8}$)	1m/s,0.3N Wear rate(mm^3/Nm) ($x10^{-9}$)	0.1m/s,0.9N Wear rate(mm^3/Nm) ($x10^{-8}$)	0.5m/s,0.9N Wear rate(mm^3/Nm) ($x10^{-8}$)	1m/s,0.9N Wear rate(mm^3/Nm) ($x10^{-9}$)
0	5.3	3.26	1.77	2.92	1.04	5.1
15	4.26	1.72	1.42	1.82	4.47	3.02
30	4.1	1.85	1.37	1.63	7.4	1.35
45	4.54	1.42	1.51	3.57	1.7	2.04
60	3.82	1.78	1.27	3.13	1.46	3.28
75	2.98	1.51	0.993	2.47	1.29	1.48
90	3.25	1.89	1.08	3.18	4.24	1.78

Table 5: Average number of wear rates in different conditions

To have a better understanding of the important controlling factor, sliding speeds. We use specific normal force 0.3N to analysis, then from the figure 37, we can conclude that the higher the speed the lower the wear rates.

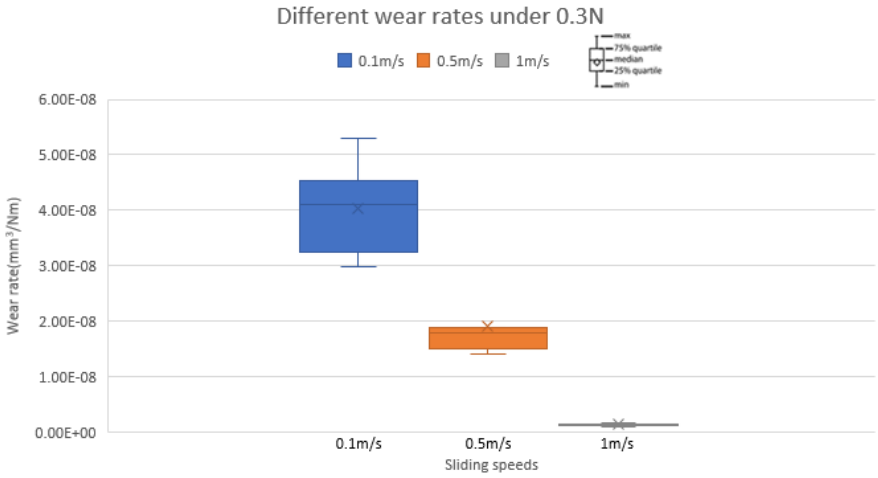

Figure 37: Wear rates in different sliding speeds under 0.3N

3.3 Further work

In the further work, I am planning to make more comparable controlling parameters like table2, and shorter the two beams of the cantilever to make it stiffer. When using SWLI, choose more degrees, like every 3 degrees to make sure more accurate data. More important, using EDS or XPS to get more surface information about the wear. And make more interesting analysis. Then we can use a more reliable outcome to excavate more properties for GaN. When using SEM, check the following things: aperture, high current, astigmatism, connection of the surface and stub, re-focus when move. Use the working distance around 5-7mm instead of 4mm when using EDS. This will give the EDS detector a better chance to detect the signal. Then we can excavate deeper to know the band bending then prove the hypothesis theoretically and try to explain.

4.Conclusion

In this thesis, for the tribological properties of GaN in relatively high speed, the COF is 0.389733 with 0.3N, 0.5m/s; 0.31119 with 0.9N, 0.5m/s; and 0.313259 with 0.9N, 1m/s. Then if we average the three number, we can get the COF is around 0.338061.

For the wear rate, in different angles, it shows around a 60 -degree period of the wear rate, the highest wear rate appears in the $< 1\bar{2}10 >$crystal direction of the GaN. On the contrary, the lowest wear rate appears in the $< 1\bar{1}00 >$direction. And in 0.5m/s, 0.3N, the wear rate reaches approximately 2×10^{-7} to $3 \times 10^{-7}\mathrm{mm}^3/Nm$, the highest wear rate for each period appears on the 0, 60, 120, 180, 240, and 300 degrees, and the lowest wear rate in the period appears on the 15,90,150,210,255,330 degrees. The highest of the wear rate in whole angles is in 180-degree, arrives on approximately $2.8 \times 10^{-7}\mathrm{mm}^3/Nm$. The lowest of the wear rate is in 90-degree, approximately $1.9 \times 10^{-7}\mathrm{mm}^3/Nm$. In 0.5m/s, 0.9N, wear rate reaches approximately 2×10^{-8} to $4 \times 10^{-8}\mathrm{mm}^3/Nm$, and it also shows around a 60-degree period. The highest of the wear rate in whole angles is in 240-degree, arrives on approximately $4.3 \times 10^{-8}\mathrm{mm}^3/Nm$. The lowest of the wear rate is in 330-degree, approximately $1.8 \times 10^{-8}\mathrm{mm}^3/Nm$. The highest wear rate for each period appears on the 0, 60, 120, 180, 240, and 300 degrees, and the lowest wear rate in the period appears on the 30,75,135,195,270,330 degrees. In 1m/s, 0.9N, the wear rate reaches approximately0.5×10^{-8} to $4 \times 10^{-8}\mathrm{mm}^3/Nm$, and it also shows around a 60-degree period. The highest of the wear rate in whole angles is in 180-degree, arrives on approximately $4 \times 10^{-8}\mathrm{mm}^3/Nm$. The lowest of the wear rate is in 135-degree, approximately $0.6 \times 10^{-8}\mathrm{mm}^3/Nm$. The highest wear rate for each period appears on the 0, 60, 105,180, 240, and 285 degrees, and the lowest wear rate in the period appears on the 45,90,135,210,270,330 degrees.

And in concluded, for the GaN, the faster the sliding speed, the lower the wear rates and the higher the normal forces, the lower the wear rates. Still, by using SEM, the higher the loads, the darker the region of the band states, which indicates different loads influence the band bending. Different sliding speeds also influence the band bending. And we hypothesis that, the higher the speeds, the more intensity of the band bending. The higher the loads, the more intensity of the band bending.

Vita

Zeyuan Tian was born on October 11th, 1994 in Xiangyang, Hubei, Chian and grew up in Wuhan, Hubei,China. He received his Bachelor of Mechanical Engineering from Wuhan Institute of Technology in Wuhan, Hubei in the summer of 2015. The following fall he began looking in internships in Hangzhou Branch, Wanxiang Group Corporation between Jul. 2015, and April 2016.Then applying Lehigh Universities in the Fall 2016 and pursuing a Master of Science in Mechanical Engineering at Lehigh University and will graduate in the May 2018.

Reference

1. peter jost. *Lubrication (Tribology) - A report on the present position and industry's needs*. (1966).

2. Tribology. *Wikipedia* (2018). Available at: https://en.wikipedia.org/wiki/Tribology.

3. Bhushan, B. *Wear*. *Introduction to Tribology* (2013). doi:10.1002/9781118403259 M4 - Citavi

4. Jost Peter, A. S. of M. E. Economic Impact of Tribology. *ASME J. Mech. Eng.***97,** 26–33 (1975).

5. Holmberg, K. & Erdemir, A. Influence of tribology on global energy consumption, costs and emissions. *Friction***5,** 263–284 (2017).

6. Sliney, H. E. & DellaCorte, C. The Friction and Wear of Ceramic / Ceramic and Ceramic / Metal Combinations in Sliding Contact. (1993).

7. Bin T, Wen Y, Zhiqiang Fu, Yanhong Gu , Chengbiao W, J. L. Microstructure and tribological properties of W-implanted PVD TiN coatings on 316L stainless steel. *Vacuum* 68–75 (2014).

8. Bin D, Ye Tao, Z. H. The microstructure, mechanical and tribological properties of TiN coatings after Nb and C ion implantation. *Appl. Surf. Sci.* 67–76 (2013).

9. Xin W, ParickY.K, David S, D.-W. Friction coefficient and sliding wear of AlTiN coating under various lubrication conditions. *Wear* 67–76 (2013).

10. Duck H. J., Kyoung M, Seung Yong S, C. S. L. Influence of ternary elements (X = Si, B, Cr) on TiAlN coating deposited by magnetron sputtering process with single alloying targets. *Thin Solid Films* (2013).

11. Fei Z, Qianzhi W, Bin Y, Xuemei W, Lanjian Z, X. C. Mechanical properties and bonding structure of boron carbon nitride films synthesized by dual ion beam sputtering. *Mater. Chem. Phys.* 215–224 (2013).

12. Pengfei W, Takanori T, Koshi A, Hiroyuki M, T. T. Preparation and tribological characterization of amorphous carbon nitride coatings in a RF PECVD-DC PVD hybrid coating process. *Appl. Surf. Sci.* 6576– 6582 (2012).

13. Chauhan, K. V. & Rawal, S. K. A Review Paper on Tribological and Mechanical Properties of Ternary Nitride based Coatings. *Procedia Technol.***14,** 430–437 (2014).

14. Vancoille E, C. J. P. and R. J. R. Mechanical properties of heat treated and worn PVD TiN, (Ti, A1)N,(Ti, Nb)N and Ti(C, N) coatings as measured by nanoindentation. *Thin*

Solid Fihns 168–176 (1993).

15. Hiroyuki H., A. K. . and T. S. Microhardness and structural analysis of (Ti,Al)N, (Ti,Cr)N, (Ti,Zr)N and (Ti,V)N films. *Vac. Sci. Technol.* (2000).

16. PalDey S., D. S. . Properties of single layer and gradient (Ti,Al)N coatings. Materials. *Mater. Sci. Eng.* 1–8 (2003).

17. Ohnuma H., Nihira N., Mitsuo A., Toyoda K.., Kubota K.., A. T. Effect of aluminum concentration on friction and wear properties of titanium aluminum nitride films. *Surf. Coatings Technol.* 623–626 (2004).

18. Wuhrer R, Y. W. . Grain refinement with increasing magnetron discharge power in sputter deposition of nanostructured titanium aluminium nitride coatings. *Scr. Mater.* 813–818 (2004).

19. Ichimiya N., Onishi Y., T. Y. Properties and cutting performance of (Ti,V)N coatings prepared by cathodic arc ion plating. Surface & Coatings Technology. *Surf. Coat. Technol.* 1377 – 1382 (2005).

20. Grzesik W., Zalisz Z., K. S. Investigations on friction and wear mechanisms of the PVD-TiAlN coated carbide in dry sliding against steels and cast iron. *Wear* 1191–1200 (2006).

21. Moa J.L, Zhua M.H, Leia B, Lenga Y.X, H. N. Comparison of tribological behaviours of AlCrN and TiAlN coatings-Deposited by physical vapor deposition. *Wear* 1423–1429 (2007).

22. Zhou Z., Rainforth W.M., Luo Q., Hovsepian P.Eh., Ojeda J.J., R.-G. M. . Wear and friction of TiAlN/VN coatings against Al2O3 in air at room and elevated temperatures. *Acta Mater.* 2912–2925 (2010).

23. Ricardo D. T. , Paulo C. Soares Jr. Cleomar S., C. J. M. S. Influence of the nitriding and TiAlN/TiN coatings thickness on the sliding wear behavior of duplex treated AISI H13 steel. *Surf. Coat. Technol.* 1381–1385 (2010).

24. Daniel K, Milan F, Pavol H, L. K. Comparative Study of Properties of Ti Based Coatings Deposited by Selected PVD Techniques. *Web Magazine MTF STU Material Science and Technology* 17–24 (2012).

25. Zhao Y.H, Hu L, Lin G.Q, Xiao J.Q, Dong C, Y. B. . Deposition, microstructure and hardness of TiN/(Ti,Al)N multilayer films. *J. Refract. Met. Hard Mater.* 27–32 (2012).

26. Xin W, ParickY.K, David S, D.-W. Friction coefficient and sliding wear of AlTiN coating under various lubrication conditions. *Wear* 67–76 (2013).

27. Yucel B. Sliding wear of CrN, AlCrN and AlTiN coated AISI H13 hot work tool steels in aluminium extrusion. *Tribol. Int.* 101–106 (2013).

28. Ipaz L. Ruiz-Luna H, Espinoza-Beltra F. J, Z. G. Correlation Between Mechanical Properties and Nanofriction of [Ti–Cr/Ti–Cr–N]n and [Ti–Al/Ti–Al–N]n Multilayers. *Tribol Lett* 403–412 (2013).

29. Radhika R., Kumar N., Pandian R., Dash S., Ravindran T.R., Arivuoli D., T. A. K. Tribological properties and deformation mechanism of TiAlN coating sliding with various counterbodies. *Tribol. Int.* 143–149 (2013).

30. Qi Z.B, Sun P, Zhu F.P, Wu Z.T, Liu B, Wang Z.C, Peng D.L, W. C. H. Relationship between tribological properties and oxidation behavior of Ti0.34Al0.66N coatings at elevated temperature up to 900 °C. *Surf. Coat. Technol.* 267–272 (2013).

31. Gallium nitride. Available at: https://en.wikipedia.org/wiki/Gallium_nitride#cite_note-8.

32. Tsao, J. Y. *et al.* Toward Smart and Ultra-efficient Solid-State Lighting. *Adv. Opt. Mater.***2,** 809–836 (2014).

33. Nelson Tansu ; Hongping Zhao ; Guangyu Liu ; Xiao-Hang Li ; Jing Zhang ; Hua Tong ; Yik-Khoon Ee. III-Nitride Photonics. *IEEE Photonics J.***2,** 241–248 (2010).

34. Crawford, M. H. LEDs for Solid-State Lighting: Performance Challenges and Recent Advances. *IEEE J. Sel. Top. Quantum Electron.***15,** 1028–1040 (2009).

35. Pust, P., Schmidt, P. J. & Schnick, & W. A revolution in lighting. *Nat. Mater.***14,** 454–458 (2015).

36. Umesh K. Mishra ; Likun Shen ; Thomas E. Kazior ; Yi-Feng Wu. GaN-Based RF Power Devices and Amplifiers. *Proc. IEEE***96,** (2008).

37. Savastenko, V. A. & Sheleg, A. U. Study of the elastic properties of gallium nitride. *Phys. Status Solidi***48,** K135–K139 (1978).

38. Deger, C. *et al.* Sound velocity of AlxGa1-xN thin films obtained by surface acoustic-wave measurements. *Appl. Phys. Lett.***72,** 2400–2402 (1998).

39. Schwarz, R. B., Khachaturyan, K. & Weber, E. R. Elastic moduli of gallium nitride. *Appl. Phys. Lett.***70,** 1122–1124 (1997).

40. Polian, A., Grimsditch, M. & Grzegory, I. Elastic constants of gallium nitride. *J. Appl. Phys.***79,** 3343–3344 (1996).

41. Majid Minary-Jolandan (a1), R. A. B. (a1) and H. D. E. Strong piezoelectricity in individual GaN nanowires. *Mater. Res. Soc.***1,** 45–48 (2011).

42. Chen, C. Y. *et al.* Gallium nitride nanowire based nanogenerators and light-emitting diodes. *ACS Nano***6,** 5687–5692 (2012).

43. Christmas, U. M. E., Andreev, A. D. & Faux, D. A. Calculation of electric field and optical transitions in InGaN/GaN quantum wells. *J. Appl. Phys.***98,** (2005).

44. Bykhovski, A. D., Gelmont, B. L. & Shur, M. S. Elastic strain relaxation and piezoeffect in GaN-AlN, GaN-AlGaN and GaN-InGaN superlattices. *J. Appl. Phys.***81,** 6332–6338 (1997).

45. Ambacher, O. & Majewski, J. Pyroelectric properties of Al (In) GaN/GaN hetero-and quantum well structures. *J. Phys. …***14,** 3399–3434 (2002).

46. Huang, J. Y., Zheng, H., Mao, S. X., Li, Q. & Wang, G. T. In situ nanomechanics of GaN nanowires. *Nano Lett.***11,** 1618–1622 (2011).

47. Bernal, R. A. *et al.* Effect of growth orientation and diameter on the elasticity of GaN nanowires. A combined in situ TEM and atomistic modeling investigation. *Nano Lett.***11,** 548–555 (2011).

48. Wheeler, J. M., Niederberger, C., Tessarek, C., Christiansen, S. & Michler, J. Extraction of plasticity parameters of GaN with high temperature, in situ micro-compression. *Int. J. Plast.***40,** 140–151 (2013).

49. Kucheyev, S. O. *et al.* Nanoindentation of epitaxial GaN films. *Appl. Phys. Lett.***77,** 3373–3375 (2000).

50. Drory, M. D., Ager, J. W., Suski, T., Grzegory, I. & Porowski, S. Hardness and fracture toughness of bulk single crystal gallium nitride. *Appl. Phys. Lett.***69,** 4044–4046 (1996).

51. Nowak, R. *et al.* Elastic and plastic properties of GaN determined by nano-indentation of bulk crystal. *Appl. Phys. Lett.***75,** 2070–2072 (1999).

52. Yang, Z. *et al.* Mechanical characterization of suspended GaN microstructures fabricated by GaN-on-patterned-silicon technique. *Appl. Phys. Lett.***88,** 1–3 (2006).

53. Aida, H. *et al.* Ultraprecision CMP for sapphire, GaN, and SiC for advanced optoelectronics materials. *Curr. Appl. Phys.***12,** S41–S46 (2012).

54. Lin, M. H., Wen, H. C., Jeng, Y. R. & Chou, C. P. Nanoscratch characterization of GaN epilayers on c- and a-Axis sapphire substrates. *Nanoscale Res. Lett.***5,** 1812–1816 (2010).

55. Zeng, G., Tan, C. K., Tansu, N. & Krick, B. A. Ultralow wear of gallium nitride. *Appl. Phys. Lett.***109,** (2016).

56. Zeng, G., Sun, W., Song, R., Tansu, N. & Krick, B. A. Crystal Orientation Dependence of Gallium Nitride Wear. *Sci. Rep.***7,** 1–6 (2017).

57. Zeng, G., Tansu, N. & Krick, B. A. Moisture dependent wear mechanisms of gallium nitride. *Tribol. Int.***118,** 120–127 (2018).

58. Guosong Zeng 1,(a), Xiaofang Yang 2, Chee-Keong Tan 3, 4, Christopher J. Marvel 5, Bruce E. Koel 2, Nelson Tansu 3,(b), and Brandon A. Krick 1, C. Shear-Induced Band Bending in Gallium Nitride.

59. Erickson, G. M. *et al.* Paleo-tribology: Development of wear measurement techniques and a three-dimensional model revealing how grinding dentitions selfwear to enable functionality. *Surf. Topogr. Metrol. Prop.***4,** (2016).